

The impacts of iron limitation and ocean acidification on the cellular stoichiometry, photophysiology, and transcriptome of *Phaeocystis antarctica*

Florian Koch, ^{1*} Sara Beszteri,¹ Lars Harms,¹ Scarlett Trimborn ^{1,2}

¹Marine Biogeosciences Alfred Wegener Institute Helmholtz Zentrum für Polar und Meeresforschung, Bremerhaven, Germany

²Marine Botany, The Alfred Wegener Institute, University of Bremen, Bremen, Germany

Abstract

Phaeocystis antarctica is an integral player of the phytoplankton community of the Southern Ocean (SO), the world's largest high-nutrient low-chlorophyll region, and faces chronic iron (Fe) limitation. As the SO is responsible for 40% of anthropogenic CO₂ uptake, *P. antarctica* must also deal with ocean acidification (OA). However, mechanistic studies investigating the effects of Fe limitation and OA on trace metal (TM) stoichiometry, transcriptomic, and photophysiological responses of this species, as well as on the Fe chemistry, are lacking. This study reveals that *P. antarctica* responded strongly to Fe limitation by reducing its growth rate and particulate organic carbon (POC) production. Cellular concentrations of all TMs, not just Fe, were greatly reduced, suggesting that Fe limitation may drive cells into secondary limitation by another TM. *P. antarctica* was able to adjust its photophysiology in response to Fe limitation, resulting in similar absolute electron transport rates across PSII. Even though OA-stimulated growth in Fe-limited and -replete treatments, the slight reduction in cellular POC resulted in no net effect on POC production. In addition, relatively few genes were differentially expressed due to OA. Finally, this study demonstrates that, under our culture conditions, OA did not affect inorganic Fe or humic-acid-like substances in seawater but triggered the production of humic-acid-like substances by *P. antarctica*. This species is well adapted to OA under all Fe conditions, giving it a competitive advantage over more sensitive species in a future ocean.

In 30–50% of the world's oceans phytoplankton, biomass is low, even though concentrations of nitrate and phosphate are plentiful (de Baar et al. 2005). Rather than macronutrients, in these high-nutrient low-chlorophyll (HNLC) regions, it is the scarcity of certain trace metals (TMs), such as iron (Fe), which governs primary production and/or plankton species composition (Bertrand et al. 2007; de Baar et al. 2005; Koch et al. 2011; Martin and Fitzwater 1988). Fe is required for vital cellular processes such as carbon and nitrogen fixation, nitrate and nitrite reduction, and chlorophyll synthesis. It is also an integral part of the electron transport chain of respiration and photosynthesis (Raven et al. 1999; Behrenfeld and Milligan 2013; Twining and Baines 2013). The majority of metalloproteins, however, have yet to be discovered (Cvetkovic et al. 2010; Lelandais et al. 2016).

The Southern Ocean (SO) is the world's largest HNLC region, responsible for roughly 40% of all oceanic uptake of anthropogenic carbon (Landschutzer et al. 2015; Sabine et al. 2004) and an area where Fe limitation of phytoplankton has been reported (Martin et al. 1990; de Baar et al. 2005; Boyd and Ellwood 2010). It is also an important region, which contributes disproportionately to upwelling of deep water and formation of intermediate and bottom waters and links the Pacific, Indian, and Atlantic Oceans. The SO is thus of global importance in climate regulation, biodiversity, and biogeochemical cycles (Buesseler 1998; Lumpkin and Speer 2007).

Atmospheric CO₂ concentrations have risen sharply since the beginning of the industrial revolution and, due to anthropogenic activity, partial pressure of CO₂ (*p*CO₂) in seawater is said to increase from present day ~ 400 to 750 μ atm by the end of this century (RCP 6.0; IPCC 2014). This will be accompanied by an increase in hydrogen ions (drop in pH) by almost 100% over present-day concentrations (Wolf-Gladrow et al. 1999), a phenomenon, which has been coined ocean acidification (OA). Even though the effects of OA on varying aspects of physiology on SO phytoplankton such as growth, photosynthesis, elemental stoichiometry, and photophysiology (Boelen et al. 2011;

*Correspondence: florian.koch@awi.de

This is an open access article under the terms of the Creative Commons Attribution-NonCommercial License, which permits use, distribution and reproduction in any medium, provided the original work is properly cited and is not used for commercial purposes.

Additional Supporting Information may be found in the online version of this article.

Trimborn et al. 2017b; Yang and Gao 2012) have been investigated, changes vary with species and even between strains. A review by Petrou et al. (2016) concludes that, in general, SO phytoplankton species do not seem to benefit from OA. Also, these changes in phytoplankton physiology can be mitigated or amplified by a combination with other stressors such as Fe limitation or light (Boyd et al. 2005; Heiden et al. 2016; Hoppe et al. 2015), making the point for more mechanistic studies to tease apart the synergistic interactions of climate change (Xu et al. 2014).

One set of interactive effects are that OA may change ocean chemistry and thus the bioavailability of Fe (Millero et al. 2009). A reduced seawater pH may, for example, increase the solubility of Fe³⁺, as Fe in seawater exists 99% as bound to strong organic ligands (Rue and Bruland 1995; van den Berg 1995; Boye et al. 2001). Over the pH range of 7.5 to 9, however, the effect of OA on Fe(III)' solubility in seawater has been shown to be small (Kuma et al. 1996; Liu and Millero 2002; Fishwick et al. 2014). Shi et al. (2010) describe that the affinity of the Fe(III)-ligand complexes may be reduced and OA has been implicated as hampering high-affinity iron uptake of carbonate-sensitive phyto-ferrin in diatoms (McQuaid et al. 2018). Furthermore, increases in pCO₂ will likely alter the chemistry of organic ligands such as porphyrins, siderophores, and humic substances (Hutchins et al. 1999; Maldonado et al. 2005; Hassler et al. 2011), affecting the bioavailability of Fe and its transfer up the food chain. Laboratory experiments investigating the effects of Fe limitation are notoriously difficult due to the high risk of Fe contamination, and as such, are routinely carried out by using strong organic chelators. This practice, however, makes it difficult to tease apart direct effects of pCO₂ on seawater Fe chemistry or to assess biologically mediated changes to Fe chemical speciation (Gerringa et al. 2000).

Phaeocystis (Prymnesiophyceae) are ubiquitous phytoplankton with a global distribution. In the SO waters surrounding Antarctica, diatoms and *Phaeocystis antarctica* are responsible for large phytoplankton blooms (Arrigo et al. 1999; Smith et al. 2000). As diatoms are more efficient exporters of fixed organic carbon than nonballasted phytoplankton, such as *P. antarctica*, community composition plays a large role in determining the efficiency of the biological pump. Past laboratory research has shown that *P. antarctica* responds dramatically to Fe limitation by changing its growth rate, particulate organic carbon (POC) production, pigment composition (van Leeuwe and Stefels 1998; DiTullio et al. 2007; van Leeuwe and Stefels 2007), and photophysiology (Alderkamp et al. 2012; Strzepek et al. 2012). Two studies (Trimborn et al. 2013; Trimborn et al. 2017b) observed no changes in growth rate and POC production when *P. antarctica* was grown under elevated pCO₂ alone and in conjunction with higher irradiance. This led the authors to conclude that, as diatoms changed their growth rates and photophysiology, they may be more sensitive to the interactive effects of OA and changes in irradiance than *P. antarctica*. In contrast, Xu et al. (2014) reported a 64% and 58% reduction in POC production as well as 46% and

64% reduction in growth rate of Fe-limited and -replete cultures of *P. antarctica* (strain CCMP3314) when grown under conditions forecasted for 2100 (increased temperature, light and pCO₂). To date, however, the interactive effects of Fe limitation and changes in pCO₂ have not been investigated mechanistically for this species, and any possible effect of OA on gene regulation and Fe chemical speciation is poorly understood.

Here, we present a study investigating the effects of OA on the physiology and gene expression of the ecologically important SO species *P. antarctica* under Fe-limiting and -replete conditions. It shows that significant changes in phytoplankton physiology, such as cellular TM stoichiometry and HA-like production, occur under Fe stress, which in turn results in chemical changes of the seawater. In contrast, OA had a limited effect on the parameter assessed, suggesting that this organism is well equipped to cope with a high CO₂ world.

Material and methods

Culture conditions

In order to minimize contamination, TM clean techniques were used in all aspects of this study. Briefly, culture work was conducted in 4 L polycarbonate (PC) bottles, which had all been sequentially soaked for 1 week in 1% Citranox[®] and for 2 weeks in 1 mol L⁻¹ hydrochloric acid (high-performance liquid chromatography [HPLC] grade, Merck Millipore Corporation). Between each soaking step, the bottles were rinsed seven times with ultrapure water (Merck Millipore Corporation). Finally, the TM-cleaned equipment/bottles were air dried under a clean bench (U.S. class 100) and packed in three polyethylene (PE) bags for storage. *P. antarctica* (isolated by P. Pendoley at 68°39S, 72°21E in 1992) was grown in 0.2 μm filter-sterilized, low Fe (0.5 nmol L⁻¹) Antarctic seawater (collected at 60°32 S; 26°29 W from a depth of 20–30 m). Cultures were maintained under these conditions for at least 1 yr prior to initiation of the main experiment. For the Fe-replete treatment (henceforth referred to as "+Fe"), a TM mix (Table 1) with 4 nmol L⁻¹ Fe was added, and the concentrations of the other TMs were adjusted to maintain the ratio of the original F/2 recipe (Table 1). This was done to ensure that experiments were conducted with TM concentrations typical for Fe-replete areas of the SO. For the Fe-deplete treatments (henceforth referred to as "-Fe"), a second TM mix without Fe was used (Table 1). As suggested by Gerringa et al. (2000), in an effort to minimize the alteration of the natural seawater TM chemistry and ligands, no ethylenediaminetetraacetic acid (EDTA) was added. All cultures were maintained under 100 μmol photons m⁻² s⁻¹ on a 16 : 8 h light : dark cycle and at 2°C with the addition of F/2-based macronutrients (nitrate, phosphate, and silicate) and vitamins (Guillard and Ryther 1962). Prior to use, the macronutrients were sent over a chelex column (Chelex[®] 100, Sigma Aldrich, Merck) in order to remove any TMs. All cultures, as well as media used for dilutions, were also gently bubbled with humidified air at pCO₂ pressures

Table 1. Concentrations of total dissolved TMs (nmol L⁻¹) in the collected filtered SO water (FSOW) and final concentrations after the addition of the F/2-based metal mix with and without Fe (+Fe and -Fe, respectively).

Element	FSOW (nmol L ⁻¹)	+Fe (nmol L ⁻¹)	-Fe (nmol L ⁻¹)
Zn	58.72	58.96	58.96
Cu	2.45	2.50	2.50
Co	0.35	0.40	0.40
Mn	1.31	3.21	3.21
Fe	0.55	4.55	0.55

of either 350 or 900 μatm , henceforth referred to as “350” and “900,” corresponding to a seawater pH of 8.19 ± 0.02 and 7.80 ± 0.01 , respectively (Table 2). CO₂ gas mixtures were generated with a gas flow controller (CGM 2000, MCZ Umwelttechnik), using CO₂-free air (< 1 ppmv CO₂; Dominick Hunter) and pure CO₂ (Air Liquide Deutschland Ltd.). The CO₂ gas mixtures were regularly monitored with a nondispersive infrared analyzer system (LI6252; Li-Cor Biosciences) calibrated with CO₂-free air and purchased gas mixtures of 150 ± 10 and 1000 ± 20 ppmv CO₂ (Air Liquide Deutschland). Cultures were acclimated to each experimental condition for at least 2 weeks, during which cells were kept in mid-exponential growth by diluting with preconditioned media. For the main experiment, each treatment was grown in triplicate in dilute batch cultures. Final sampling of all treatments took place when cells were in exponential growth and had reached densities of $1\text{--}1.5 \times 10^5$ cells/mL, ensuring stable carbonate chemistry (Table 2). This particular strain of *P. antarctica* does not form colonies, thus changes in cell densities were determined daily, using a Beckman Multisizer™ 3 Coulter Counter® with a 100 μm aperture. Growth rates, μ (d⁻¹), were calculated from:

$$\mu = \ln(N_t : N_0) / t$$

where N_0 and N_t are at the end and start of exponential-phase of growth, respectively, while t is the duration of the exponential growth phase.

Table 2. Carbonate chemistry determined at the end of the experiment for *P. antarctica* grown under iron replete (+Fe) and limited (-Fe) conditions when exposed to ambient (350 μatm) and elevated (900 μatm) partial pressure of carbon dioxide ($p\text{CO}_2$) levels. $p\text{CO}_2$ was calculated from the measured pH (National Bureau of standards [NBS] scale) and alkalinity. Concentrations of DIC were also determined and are shown here, but they were not used for $p\text{CO}_2$ calculation. All values are mean \pm standard deviation.

Treatment		pH (NBS)	Alkalinity ($\mu\text{mol kg}^{-1}$)	DIC ($\mu\text{mol kg}^{-1}$)	$p\text{CO}_2$ (μatm)
$p\text{CO}_2$	Fe				
350	+	8.19 ± 0.02	2319 ± 4	2176 ± 2	345 ± 15
	-	8.20 ± 0.03	2309 ± 2	2168 ± 7	327 ± 26
900	+	7.80 ± 0.01	2325 ± 3	2279 ± 2	899 ± 25
	-	7.81 ± 0.01	2349 ± 31	2286 ± 3	899 ± 21

Determination of carbonate chemistry

The pH was monitored every 2 d using a pH-Meter 827 (Metrohm), calibrated using a three-point calibration (National Institute of Standards and Technology certified buffers). The pH was stable (deviations < 0.05 pH units), being 8.19 ± 0.02 and 7.80 ± 0.01 for 350 and 900, respectively (Table 2). Samples for dissolved inorganic carbon (DIC) and total alkalinity (TA) were filtered through 0.2 μm filter cartridges (Nalgene, Thermo Scientific) or glass fiber filters, respectively. DIC was stored at 4°C in 5 mL gas-tight borosilicate bottles without headspace until subsequent colorimetric analysis on a QuAatro autoanalyzer (Seal Analytical, Stoll et al. 2001). TA was stored at 4°C and was measured via potentiometric titration (Brewer et al. 1986), and concentrations were calculated using a linear Gran Plot (Gran 1952). Certified reference material was used to correct for instrument error (A. Dickson, SIO). Dissolved inorganic nutrients were frozen at -20°C until subsequent analysis on a QuAatro39 AutoAnalyzer (Seal Analytical GmbH) following standard colorimetric analysis. The $p\text{CO}_2$ was calculated based on TA, pH, concentrations of phosphate and silicate, temperature, and salinity using the CO2Sys program (Table 2; Pierrot et al. 2006) choosing the equilibrium constants of Mehrbach et al. (1973) as refitted by Dickson and Millero (1987).

Determination of TM and ligand chemistry

All labware used for analysis was precleaned according to the Geotrace cookbook (Cutter et al. 2017). Prior to the analysis of trace elements, 0.2 μm prefiltered seawater samples were acidified to pH 1.75 with double distilled HNO₃ and UV oxidized using a 450 W photochemical OV power supply (ACE GLASS Inc.). Two blanks were processed the same way during each UV digestion step. Total dissolved Fe, Mn, Zn, Co, and Cu concentrations of seawater samples and process blanks were analyzed using a seaFAST system (Elemental Scientific; Hathorne et al. 2012) coupled to a sector field inductively coupled plasma mass spectrometry (ICP-MS; Element 2, Thermo Fisher Scientific; resolution of $R = 4000$). The ICP-MS was optimized daily to achieve oxide forming rates below 0.3%. Each seawater sample was analyzed via standard addition, to minimize any matrix effects, which might influence

the quality of the analysis. The pH of 1.75 was needed, in order to minimize the formation of Mn and Fe hydroxides, and was sufficiently high to minimize the loss of other TMs on the SeaFast column (Hr. Klemens, pers. Comm., ESI). To assess the accuracy and precision of the method, a NASS-6 (National Research Council of Canada) reference standard was analyzed in a 1 : 10 dilution (corresponding to environmentally representative concentrations) at the beginning, in between and at the end of a run (two batch runs; $n = 6$), yielding recovery rates between 95% and 101%.

Dissolved humic acid (HA)-like substances ($< 0.2 \mu\text{m}$, HA-like), as well as the chemical speciation of Fe were analyzed using cathodic stripping voltammetry (CSV; Croot and Johansson 2000, Laglera et al. 2007, Abualhaija and van den Berg 2014). Specifically, HA-like compounds were measured via electrochemical measurements on a VA-Stand 663 coupled to a AUTOLAB PGSTAT 101 (Metrohm) with a hanging mercury drop electrode (HMDE drop size 2, $0.4 \text{ mm}^2 \pm 10$), a glassy carbon rod counter electrode, and a double junction Ag/AgCl reference electrode with a salt bridge filled with 3 M KCl. About 500 μL of a mixed reagent solution consisting of 0.4 M KBrO₃ 0.4 M (Sigma), 0.2 M 4-(2-hydroxyethyl)-1-piperazinepropanesulfonic acid (EPPS, Sigma) and 0.2 M NH₄OH (Seastar) and 50 nM FeCl₃ (ICP-MS Standard, Fluka) were added to 10 mL of sample in order to obtain a pH of 8.2 and saturate the natural HA-like compounds with Fe. The samples were then allowed to react for at least 2 h in the dark, followed by 4 min of deaeration using high purity argon followed by a 2–5 min deposition time. Concentrations of HA-like were quantified using internal standard additions of Suwanne River fulvic acid (SRFA standard I, International Humic Substances Society) and are expressed as $\mu\text{g L}^{-1}$ SRFA equivalent. Standards were prepared monthly and stored at 4°C in the dark. The detection limit of the instrument was 3.7 $\mu\text{g L}^{-1}$ SRFA equivalent using a 3 min deposition time. For hardware operation and data analysis, Autolab NOVA version 1.17 used and HA-like concentrations calculated according to Laglera and van den Berg (2009). Finally, HA-like concentrations for culture treatments were normalized to cell numbers and incubation time to yield HA-like production rates as $\text{fg cell}^{-1} \text{d}^{-1}$. The chemical speciation of Fe was determined using competitive ligand exchange adsorptive CSV using 10 μM of the ligand 2-(2-thiazolylazo)-*p*-cresol (TAC, LOT 30549, Alfa Aesar) according to Croot and Johansson (2000). Defrosted samples were split into 10 mL subsamples and buffered with 5 mM EPPS to obtain a pH of 8.1. Variable amounts of a 0,75 μM Fe standard were added in order to obtain concentrations between 0 and 6 nM added Fe. After 2 h of equilibration, the TAC was added and sample analysis was conducted 24 h later. Before measuring on a bioanalytical system consisting of an EC epsilon potentiostat and a controlled growth mercury electrode, the titration cell was preconditioned three times with the mixed reagent solution. As a working electrode, a medium mercury drop (size 8) was used in conjunction with the static mercury drop electrode setting, an Ag/AgCl reference electrode and a platinum wire counter electrode. A titration against

diethylene triamine pentaacetic determined an α of 327 prior to sample analysis. Fe chemical speciation was calculated according to nonlinear fit method of Gerringa et al. (1995) and the linearization model of van den Berg (1982).

In order to separate OA-induced changes in the chemistry from those induced by biological processes, abiotic (no addition of culture) control bottles for each treatment (350+Fe, 350-Fe, 900+Fe, and 900-Fe) were incubated alongside the main experiment, and sampled for carbonate chemistry, dissolved TMs, dissolved inorganic Fe, and HA-like, as described before.

Cellular carbon, nitrogen, and TM quotas

POC and particulate organic nitrogen (PON) was measured by capturing cells on precombusted (15 h, 500°C) GF/F filters (nominal pore size 0.7 μm ; Whatman). Filters were stored at -20°C, acidified with 200 μL of 0.2 N HCl and dried for > 12 h at 55°C prior to analysis on an Euro Elemental Analyzer 3000 CHNS-O (HEKAtech GmbH). Combusted filters were run as blanks, subtracted and POC/PON values normalized to cell densities, yielding cellular quotas. POC and PON production was calculated by multiplying cellular POC/PON contents by the growth rate. Phytoplankton cells were collected on 0.2 μm TM clean PC filters (EMD Millipore) and rinsed with an oxalic acid wash (Hassler and Schoemann 2009) to remove TMs bound to the cell surface. Finally, the filters were rinsed with filtered seawater and placed into TM-cleaned 25 mL poly(fluor alkoxy) vials. Intercellular TM contents were subsequently analyzed via ICP-MS following a digestion with HNO₃ and HF (Ho et al. 2003; Twining and Baines 2013). All filters were digested for 16 h at 180°C using 5 mL of subboiled HNO₃ (distilled 65%, p.a., Merck) and 0.5 mL of sub-boiled HF (40%, suprapure, Merck) followed by the addition of 0.5 mL of Milli-Q water. Under a glass hood, the volume of the cell extract was concentrated to 0.5 mL via evaporation on a 140°C hot plate and the evaporate was passed through a Ca(OH)₂/NaOH solution, which effectively neutralized it. About 0.2 mL of subboiled HNO₃ (distilled 65%, p.a., Merck) was then added, and the solution was transferred into 10 mL TM cleaned polypropylene vials. Finally, 10 μL of Rh (1 mg L⁻¹) was added as an internal standard, and the volume was brought up to 10 mL using Milli-Q water before subsequent analysis on a high resolution ICP-MS (Attom, Nu Instruments). Acid (5 mL of sub-boiled HNO₃, 0.5 mL HF) and two filter blanks as well as the BCR-414 (Plankton reference material, Sigma Aldrich) samples were also processed and analyzed in order to assure low background TM values as well as digestion quality (Supporting Information Table S1). Intracellular TM contents were then normalized per cell or POC.

Pigment analysis

Pigment concentrations were collected on GF/F filters, flash frozen in liquid nitrogen, and stored at -80°C in the dark. Before analysis, pigments were extracted for 24 h at 4°C in the

dark, using 90% acetone. Following centrifugation (5 min, 4°C, 13,000 rpm) and filtrations through a 0.45 µm pore sized syringe filter, concentrations of the light harvesting (LH) pigments chlorophyll *a* (Chl *a*) and *c*₂ (Chl *c*₂), fucoxanthin (Fuco), and the light protective (LP) pigments diatoxanthin (Dt) and diadinoxanthin (Dd) were determined by reverse phase HPLC on a LaChromElite® system equipped with a chilled autosampler L-2000 and a DAD detector L-2450 (VWR-Hitachi International GmbH). For the separation of the pigments, a solvent gradient was applied to a Spherisorb® ODS-2 column (25 cm × 4,6 mm, 5 µm particle size; Waters) with a LiChropher® 100-RP-18 guard cartridge (Wright et al. 1991). Peaks were identified, quantified against known concentrations of standards for the pigments in question (DHI Lab Products), and analyzed using the EZChrom Elite (Ver. 3.1.3.; Agilent Technologies).

Photosynthetic parameters

Treatment effects on the photophysiology of *P. antarctica* were assessed with a fast repetition rate fluorometer in combination with a FastAct Laboratory system (FastOcean PTX), both from Chelsea Technologies Group Ltd. All measurements were taken at 2°C following a 10 min dark acclimation period, assuring that all photosystem II (PSII) reaction centers were fully oxidized and nonphotochemical quenching (NPQ) was relaxed (Trimborn et al. 2013; Trimborn et al. 2017b). Excitation wavelength of the fluorometer's LED was 450 nm with an automated adjustment of the light intensity to 0.66–1.2 × 10²² µmol photons m⁻² s⁻¹. A single turnover mode with 100 flashlets saturation phase on a 2 µs pitch and 40 flashlets relaxation phase on a 40 µs pitch was used to increasingly saturate PSII. Iterative algorithms for the induction (Kolber et al. 1998) and relaxation phases (Oxborough et al. 2012) were applied to estimate minimum Chl *a* fluorescence (F_0) and maximum Chl *a* fluorescence (F_m). The apparent maximum quantum yield of photosynthesis of PSII (F_v/F_m) could then be calculated according to the equation

$$F_v/F_m = (F_m - F_0)/F_m$$

Photosynthesis-irradiance-curve (PE-curves) were generated using nine levels of irradiances between 0 and 1400 µmol photons m⁻² s⁻¹ with a 5 min acclimation to each light level followed by six subsequent Chl *a* fluorescence measurements at each light level. From these measurements, the light-adapted minimum (F') and maximum (F_m') fluorescence of the single turnover acquisition was estimated. The effective PSII quantum yield under ambient light (F_q'/F_m') was derived according to the equation $(F_m' - F')/F_m'$ (Genty et al. 1989). Absolute electron transport rates (aETR, e⁻ PSII⁻¹ s⁻¹) for each light level were calculated from $\sigma_{\text{PSII}} \times [(F_q'/F_m')/(F_v/F_m)] \times E$ (Suggett et al. 2009; Huot and Babin 2010; Schuback et al. 2015), where σ_{PSII} is the functional absorption cross section of PSII's photochemistry (nm²) and E denotes the instantaneous irradiance (photons

m⁻² s⁻¹). In addition, the aETR was multiplied by the concentration of RCIIIs, resulting a cellular ETR (nETR; amol e⁻ cell⁻¹ s⁻¹). The aETRs vs. irradiances were then curve fitted according to Ralph and Gademann (2005), which takes into account possible photoinhibition, and photosynthetic parameters, including minimum saturating irradiance (I_k), the potential maximum aETR (aETR_{max}), and the maximum light utilization efficiency (α). Following the PE-curve, the F_v/F_m was determined once more, after an additional 10 min dark acclimation, to assess potential damage to the photosystems. This was termed "yield recovery," consisting of the ratio of F_v/F_m measured before and after the PE curve expressed as percent (Heiden et al. 2016). NPQ was calculated following the Stern-Volmer equation:

$$\text{NPQ} = F_m/F_m' - 1$$

Additionally, the time constant for electron transport at the acceptor side of PSII (τ_{Qa} , µs), the connectivity factor of adjacent PSII LH complexes (P , dimensionless) and the concentration of functional PSII reaction centers, which was normalized to per cell ([RCII], amol cell⁻¹), were obtained using the FastPro8 software (Version 1.0.50, Kevin Oxborough, CTG Ltg.) as described by Oxborough et al. (2012).

Statistical analysis

To assess the impacts of OA and Fe limitation and evaluate any potential synergistic effects of the two environmental factors on *P. antarctica*, differences of the various parameters measured were statistically analyzed using two-way analysis of variance (ANOVA). The $p\text{CO}_2$ level and Fe depletion/enrichment were treatment factors, and a $p < 0.05$ was used to establish significant differences among treatments. The level of significance was chosen as $\alpha = 0.05$.

RNA extraction and analysis

P. antarctica cells were gently filtered onto 0.2 µm PC filters, resuspended in lysis buffer, shock frozen in liquid nitrogen, and kept at -80°C until total RNA extraction. For the latter a RNeasy Plant Mini Kit (Qiagen) was used according to manufacturer's instructions. The quantity and quality of the RNA was monitored using a NanoDrop ND-1000 spectrophotometer (Pqlab) and Agilent 2100 Bioanalyzer (Agilent), respectively. Paired-end sequencing of 50 base pairs was performed on a HiSeq 2000 sequencer, utilizing the Illumina chemistry (European Molecular Biology Laboratory). Raw reads were quality controlled by FastQC v. 0.10.01 (Babraham Institute). The quality of the reads was further improved by applying the following filter parameters using Trimmomatic v. 0.32 (Bolger et al. 2014): leading 3, trailing 3, sliding window 4:15 minlen 36. The sequencing data was de novo assembled using the Trinity genome-independent transcriptome assembler (release 2.0.4; Grabherr et al., 2011) with a minimum contig length of 200 bases. Functional annotation was performed using the Trinotate functional annotation suite (release 2.0.1; Grabherr

et al. 2011). The complete list of functional annotations with an e-value $\leq 10^{-9}$ can be seen in Supporting Information Data S1. For differential expression analysis, short reads of each sample were separately aligned against the de novo reference transcriptome, using Bowtie v. 1.0.0 (Langmead et al. 2009). Relative abundances were estimated by RSEM v. 1.2.11 (Li and Dewey 2011). Genes were analyzed for differential expression using the edgeR (Robinson et al., 2010) with a standard level of $p < 0.001$ and a fold change of at least 2 indicating significance. Tools were executed using the trinity package release 2.0.4 (Grabherr et al., 2011).

Results

Both OA and Fe depletion resulted in significant changes in the physiology of *P. antarctica*, although these changes were more pronounced for -Fe compared to OA. There were few interactive effects of the two environmental variables, with those observed pertaining mostly to photophysiology and the production of HA-like substances.

Cell size and growth rates

Cell size was significantly affected by -Fe ($p < 0.001$), resulting in a 28% reduction of cell volume in 350 (9.20 ± 0.32 to $6.57 \pm 0.26 \mu\text{m}^3$ for +Fe and -Fe, respectively) and 900 (8.66 ± 0.42 to $6.94 \pm 0.28 \mu\text{m}^3$ for +Fe and -Fe, respectively; Fig. 1a). As a consequence the surface area to volume ratio (SA/V) increased significantly from 3.4 ± 0.04 and 3.5 ± 0.05 in +Fe (350 and 900, respectively; Supporting Information Table S2) to 3.8 ± 0.05 and 3.7 ± 0.05 in -Fe (350 and 900, respectively; Supporting Information Table S2). OA did not change the cell size for +Fe or -Fe. Although growth rates were significantly lower in the -Fe compared to the +Fe treatments for both $p\text{CO}_2$ treatments (Fig. 1b), OA resulted in a significant increase in growth rates (0.24 ± 0.02 vs. $0.26 \pm 0.02 \text{ d}^{-1}$ and $0.36 \pm 0.03 \text{ d}^{-1}$ vs. 0.40 ± 0.02) in the -Fe and +Fe of 350 and 900, respectively; $p < 0.001$; Fig. 1b).

POC/PON production

Under -Fe conditions, POC per cell was significantly ($p < 0.001$) lower (3.96 ± 0.08 and $3.60 \pm 0.23 \text{ pg cell}^{-1}$ for 350 and 900, respectively; Fig. 1c) than +Fe conditions (5.67 ± 0.45 and $4.65 \pm 0.08 \text{ pg cell}^{-1}$ for 350 and 900, respectively; Fig. 1c). OA ($p = 0.005$) alone decreased the cellular carbon content by 18% and 10% in +Fe and -Fe, respectively, with OA and -Fe having a synergistic effect and resulting in the lowest POC values of any treatment (35% in 900-Fe than 350 + Fe; Fig. 1c). POC production values at 350 (2.04 ± 0.05 and $0.98 \pm 0.09 \text{ pg cell}^{-1} \text{ d}^{-1}$ for +Fe and -Fe, respectively; Fig. 1d) and 900 (1.86 ± 0.12 and $0.94 \pm 0.03 \text{ pg cell}^{-1} \text{ d}^{-1}$ for +Fe and -Fe, respectively; Fig. 1d) revealed a significant ($p < 0.001$) decrease in response to Fe limitation, while OA had no effect in all Fe treatments (Fig. 1d). -Fe or OA did not

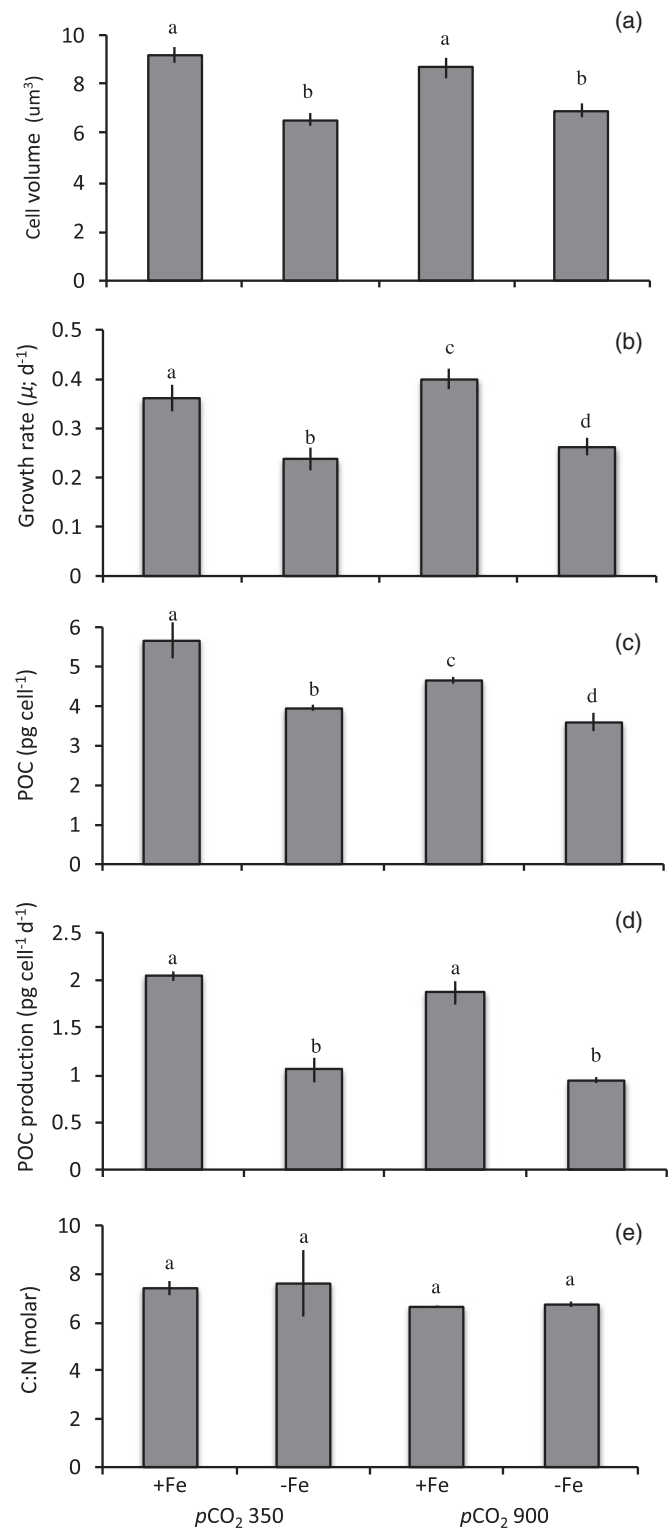


Fig. 1. Effects of iron (Fe) limitation and increased $p\text{CO}_2$ on cell volume (a), growth rate (b), POC (c) quota, POC-production (d), and molar carbon : nitrogen (C : N; e) ratios of *P. antarctica*. Cultures were grown under iron deplete (-Fe) and replete (+Fe) conditions and exposed to ambient (350 μatm) and elevated (900 μatm) $p\text{CO}_2$. Data shown represent mean \pm standard deviation ($n = 3$). Statistical differences (two-way ANOVA, $p < 0.05$) are denoted by varying small letters.

have significant effects on the molar carbon : nitrogen ratio (C : N) of *P. antarctica* (Fig. 1e).

Intracellular TM quotas

Fe limitation of *P. antarctica* resulted in a dramatic decrease ($p < 0.001$) of carbon normalized TM quotas of cells grown at 350 (15.4 ± 4.1 vs. 328 ± 96.1 amol Fe cell⁻¹, 1.03 ± 0.02 vs. 653 ± 208 amol Zn cell⁻¹, 0.64 ± 0.19 vs. 11.9 ± 9.58 amol Cu cell⁻¹, 0.64 ± 0.55 vs. 5.46 ± 0.16 amol Mn cell⁻¹, 1.56 ± 0.02 vs. 1.94 ± 0.21 amol Co cell⁻¹) in the -Fe vs. the +Fe treatment (Fig. 2a,b). Similarly, under 900, -Fe vs. +Fe treatment caused a decrease of the carbon normalized cellular Fe (20.2 ± 18.9 vs. 360 ± 92.4 amol cell⁻¹; Fig. 2a), Zn (11.6 ± 9.50 vs. 878 ± 219 amol cell⁻¹; Fig. 2a), Cu (0.86 ± 0.31 vs. 12.5 ± 4.33 amol cell⁻¹; Fig. 2b), and Co (0.32 ± 0.07 vs. 2.03 ± 0.65 amol cell⁻¹; Fig. 2b) while Mn (1.51 ± 0.60 vs. 2.15 ± 0.93 amol cell⁻¹; Fig. 2b) was similar. OA resulted in a significant decrease of all cellular TMs besides Zn for the +Fe treatments (Supporting Information Table S3), but had no significant effect on carbon normalized TM quotas (Fig. 2).

Pigment composition

Under Fe limitation, all of the quantified LH pigment concentrations (Total LH) decreased significantly (35% and 43% for 350 and 900, respectively; $p < 0.01$; Table 3). Fe limitation resulted in a significant decline in cellular concentrations of Chl *a*, Chl *c*₂, and Fuco in both *p*CO₂ treatments ($p < 0.001$; Table 3).

OA did not have a significant effect on any of the quantified LH pigments. In contrast to total LP and Dt, Dd was the only pigment measured, where concentrations were not affected by Fe limitation. In response to elevated *p*CO₂, however, total LP and Dt contents decreased significantly ($p < 0.011$) while Dt was unaffected (Table 3). The ratio of Dt/Dd increased significantly under -Fe and remained unchanged by OA (Table 3).

Photophysiology

Given the central role of Fe in photosynthesis, it was not surprising that the -Fe treatments significantly affected the photophysiology of *P. antarctica*. The photosynthetic yield (F_v/F_m) was significantly ($p < 0.001$) lower in the -Fe (0.26 ± 0.02 and 0.29 ± 0.02 for 350 and 900, respectively) than the +Fe treatments (0.42 ± 0.01 and 0.41 ± 0.01 for 350 and 900, respectively), indicating that cultures in the -Fe treatments were indeed Fe limited (Table 4). In contrast, OA did not have any impact on F_v/F_m values. The absolute maximum electron transport rates ($aETR_{max}$) were affected by -Fe, with a two way ANOVA revealing a significant ($p < 0.01$) 13% increase for all -Fe treatments over all +Fe. An OA effect, however, was found (Fig. 3a,b, Table 4). α , a measure of the organism's photosynthetic efficiency at low (sub- I_k) irradiances, was significantly ($p < 0.026$) affected by -Fe, with the 900-Fe treatment having a 20% higher α than the 900 +Fe (Table 4). However, significant OA effects for

this parameter were not observed. The minimum saturating irradiances (I_k), the irradiance where ETR is 50% of $aETR_{max}$, was similar for 350+Fe and 350-Fe (95.2 ± 4.8 and 95.6 ± 2.8 $\mu\text{mol photons m}^{-2} \text{s}^{-1}$, respectively) while Fe limitation resulted in a significant ($p = 0.003$) increase in the 900 treatments (77.4 ± 4.7 and 87.4 ± 6.2 $\mu\text{mol photons m}^{-2} \text{s}^{-1}$) for +Fe and -Fe, respectively (Fig. 3a,b, Table 4). OA, on the other hand, resulted in a slightly significant ($p = 0.04$) reduction in both the +Fe and -Fe treatments. These trends were mirrored when multiplying $aETR$ by the [RCII].

Nonphotochemical quenching

In comparison to -Fe conditions, NPQ was nearly 75% lower for higher irradiances under Fe replete conditions and followed a saturation curve (Fig. 3c,d). In contrast, NPQ increased nearly linearly with no clear saturation even at the high irradiances under Fe limiting conditions. No OA effects were observed for any Fe treatment.

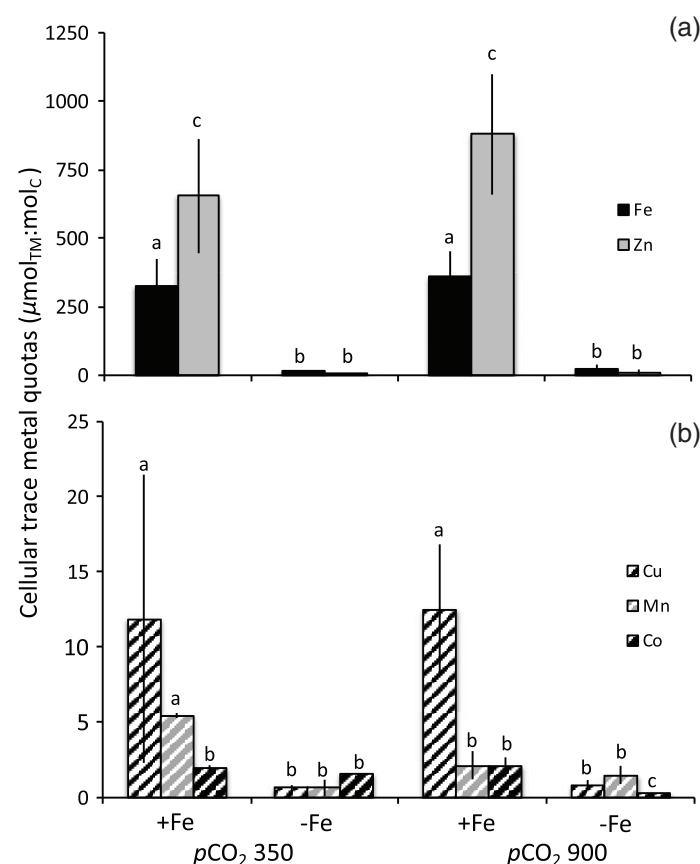


Fig. 2. Effects of iron (Fe) limitation and increased *p*CO₂ on the intracellular TM stoichiometry of *P. antarctica*. Carbon normalized quotas of the TMs iron and zinc (Fe and Zn, respectively; **a**), as well as copper (Cu), manganese (Mn), and cobalt (Co; **b**). cultures were grown under iron deplete (-Fe) and replete (+Fe) conditions, exposed to ambient (350 μatm) and elevated (900 μatm) *p*CO₂. Data shown represent mean \pm standard deviation ($n = 3$). Statistical differences (two-way ANOVA, $p < 0.05$) are denoted by varying small letters.

Table 3. Cellular concentrations of total LH pigments (Total LH), Chl *a*, Chl *c*₂, Fuco, total LP pigments (total LP), Dd, Dt concentrations, and the Dt/Dd ratio for *P. antarctica* grown under iron replete (+Fe) and iron limited (-Fe) conditions and exposed to ambient (350 μatm) and elevated (900 μatm) $p\text{CO}_2$. Values represent mean \pm standard deviation ($n = 3$). Negative changes in pigment concentrations and their degree of significance (p , two-way ANOVA) due to Fe limitation or increased $p\text{CO}_2$ is given in the two right columns (“-Fe effect” and “OA effect,” respectively).

Pigment (fg cell ⁻¹)	350 μatm $p\text{CO}_2$		900 μatm $p\text{CO}_2$		-Fe effect	OA effect
	+Fe	-Fe	+Fe	-Fe		
	LH					
Total LH	73.8 \pm 5.23	53.4 \pm 2.13	76.2 \pm 3.93	49.2 \pm 5.55	< 0.001	
Chl <i>a</i>	42.0 \pm 1.9	26.8 \pm 1.4	42.1 \pm 2.1	24.7 \pm 1.6	< 0.001	
Chl <i>c</i> ₂	8.4 \pm 0.8	5.1 \pm 0.7	8.5 \pm 0.6	3.7 \pm 3.2	< 0.001	
Fuco	22.5 \pm 2.6	21.3 \pm 0.6	24.9 \pm 1.4	20.6 \pm 0.9	0.017	
	LP					
Total LP	8.92 \pm 0.97	7.38 \pm 0.54	7.19 \pm 0.31	6.69 \pm 0.29	< 0.001	0.012
Dd	8.16 \pm 0.97	7.18 \pm 0.54	6.56 \pm 0.31	6.53 \pm 0.29		0.011
Dt	0.75 \pm 0.05	0.21 \pm 0.00	0.63 \pm 0.01	0.16 \pm 0.02	0.001	
Dt/Dd	0.07 \pm 0.01	0.05 \pm 0.00	0.08 \pm 0.00	0.05 \pm 0.01	0.001	

Changes to PSII

The connectivity between PSII (P) decreased by 60% due to Fe limitation in 350 while no Fe effect was observed in 900 ($p < 0.001$ for 350; Fig. 4a). Conversely, OA resulted in a $\sim 20\%$ decline in the +Fe and a $\sim 45\%$ increase in the -Fe treatments ($p < 0.048$ and 0.002 for +Fe and -Fe, respectively). The functional absorption cross section of PSII (σPSII) increased significantly under -Fe at both $p\text{CO}_2$ levels ($p = 0.014$; Fig. 4b). Under OA, σPSII was similar for the +Fe treatments, but increased under -Fe ($p = 0.012$; Fig. 4b). In contrast to σPSII , the concentration of functional reaction centers for PSII per cell ([RCII]) was not affected by -Fe (Fig. 4c) or OA (Fig. 4a). Finally, *P. antarctica* did not respond to -Fe by changing the time constant for electron transport on the accelerator side of PSII (τ) under 350 while at 900 τ treatment declined by 22% under Fe limitation, indicating a significant interactive effect of Fe limitation and OA ($p = 0.006$; Fig. 4d).

Fe chemistry

The concentration of total dissolved Fe (Fe dissolved) and inorganic Fe (Fe') in the abiotic controls (seawater without *Phaeocystis*) were significantly ($p < 0.001$ for 350 and 900) higher in the +Fe compared to the -Fe treatments irrespective of the $p\text{CO}_2$, whereas concentrations of HA-like remained the same (Fig. 5a-c). For all abiotic controls, OA did not result in changes in concentrations of total Fe dissolved, Fe' or HA-like. Compared to the abiotic controls, concentrations of Fe dissolved in the incubation bottles with *P. antarctica* were significantly lower in the +Fe, but similar for the -Fe treatments at both $p\text{CO}_2$ levels ($p < 0.001$; Fig. 5a). Again, OA did not result in a significant change. In the incubation bottles with *P. antarctica*, Fe' concentrations were significantly lower than their respective abiotic controls (Fig. 5b). Under 350, Fe' concentrations of the incubation bottles with *P. antarctica* were 0.25 ± 0.11 and 0.34 ± 0.12 pmol L⁻¹ for +Fe and -Fe,

Table 4. Photophysiological parameters for *P. antarctica* grown under iron-replete (+Fe) and -limited (-Fe) conditions, exposed to ambient (350 μatm) and elevated (900 μatm) $p\text{CO}_2$. F_v/F_m denotes the photosynthetic yield, $a\text{ETR}_{\text{max}}$ is the maximal absolute electron transport rate, while α represents the slope of the photosynthesis irradiance (PI) curve under light limiting conditions. I_k denotes the light intensity, at which electron transport is 50% of $a\text{ETR}_{\text{max}}$. The yield recovery represents the F_v/F_m measured after the exposure to the light range of the PI curve normalized to the initial F_v/F_m . Values represent mean \pm standard deviation ($n = 3$). Statistically significant differences (two-way ANOVA, $p < 0.05$) are denoted by varying small symbols.

	350 μatm $p\text{CO}_2$		900 μatm $p\text{CO}_2$	
	+Fe	-Fe	+Fe	-Fe
F_v/F_m (rel. Unit)	0.42 \pm 0.01*	0.26 \pm 0.02†	0.41 \pm 0.02*	0.29 \pm 0.03†
$a\text{ETR}_{\text{max}}$ (e ⁻ PSII ⁻¹ s ⁻¹)	329 \pm 71*†	359 \pm 41*†	266 \pm 31*	415 \pm 25†
α (rel. Unit)	3.6 \pm 0.6*	3.8 \pm 0.5*	3.4 \pm 0.4*	4.77 \pm 0.8*
I_k ($\mu\text{mol photons m}^{-2} \text{s}^{-1}$)	95 \pm 4*	95 \pm 2*	77 \pm 4†	87 \pm 6†*
Yield recovery (%)	54 \pm 0*	36 \pm 4†	44 \pm 3‡	31 \pm 1†

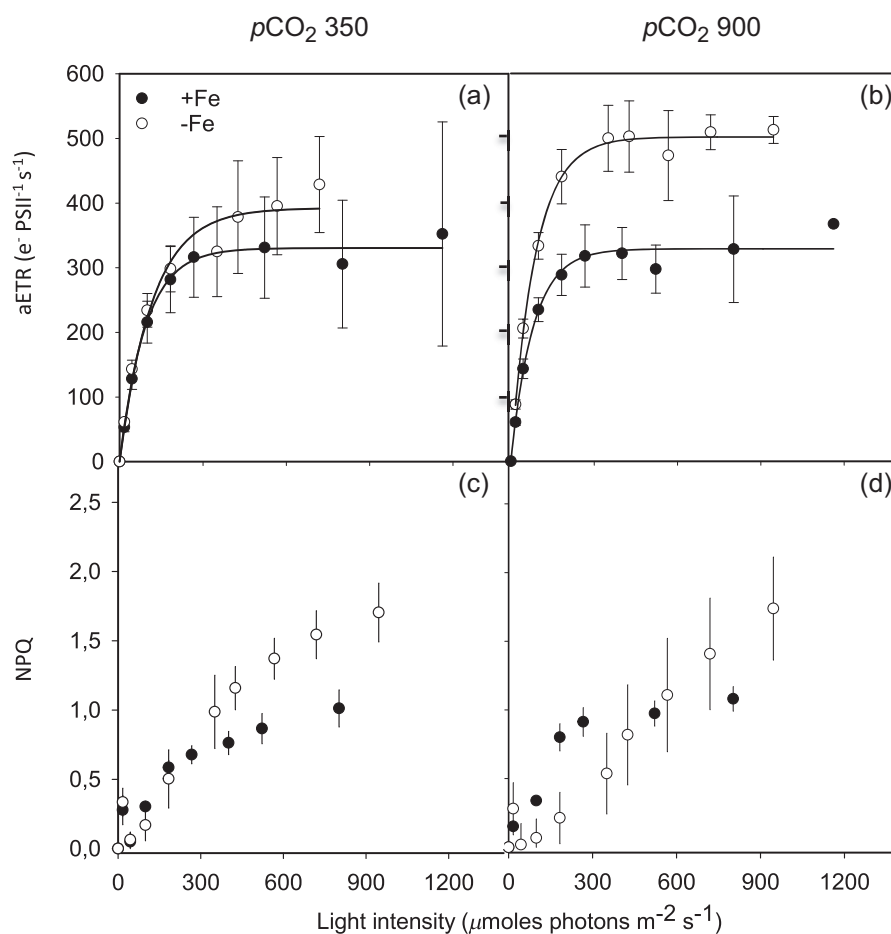


Fig. 3. Effects of iron (Fe) limitation and increased $p\text{CO}_2$ on absolute electron transport rates (aETR, $e^- \text{PSII}^{-1} \text{s}^{-1}$; **a, b**) and nonphotochemical quenching (NPQ, relative units; **c, d**) for *P. antarctica* in response to increasing instantaneous irradiance. Cultures were grown in iron replete (+Fe, dark circles) and limited (-Fe, open circles) conditions under ambient (350 μatm ; **a, c**) and elevated (900 μatm ; **b, d**) $p\text{CO}_2$. Data represent mean \pm standard deviation ($n \geq 4$).

respectively. Unlike Fe dissolved and Fe' , concentrations of HA-like substances were significantly ($p < 0.05$) higher in the cultures (65 ± 3.73 , 32.85 ± 6.39 , 21.44 ± 4.35 , and $47.38 \pm 3.05 \mu\text{g L}^{-1}$ for 350+Fe, 350-Fe, 900+Fe, and 900-Fe, respectively) compared to their abiotic controls. The latter were the same ($p > 0.05$) for all treatments ($17.71 \pm 3.09 \mu\text{g L}^{-1}$; pooled mean \pm standard deviation), indicating that the cells were actively producing HA-like. There was a significant Fe limitation effect at 350, with HA-like production rates declining from 75.15 ± 9.91 to $12.09 \pm 1.82 \text{ fg cell}^{-1} \text{ d}^{-1}$ for +Fe and -Fe, respectively ($p < 0.001$; Fig. 5c). The same trend was observed at 900, with HA-like production rates decreasing from 26.15 ± 6.16 to $18.59 \pm 2.35 \text{ fg cell}^{-1} \text{ d}^{-1}$ for +Fe and -Fe, respectively ($p < 0.001$; Fig. 5c). While no OA effects were observed in the abiotic controls, production of HA-like substances decreased 75% ($p < 0.001$) in the +Fe incubation bottles from 350 to 900, but remained similar for the -Fe in the treatments containing *P. antarctica* cells (Fig. 5c).

Gene expression

After assembly and quality check, 57,847 genes were identified in the transcriptome of *P. antarctica*. Exact tests, applying the cutoffs $p < 0.001$ and a fold change of two, were performed to identify differentially expressed genes. In total, 1739 genes were identified, with $< 30\%$ of them being differentially expressed and annotated based on similarity searches against existing databases (Supporting Information Data S1). Of these, 42% were categorized as "poorly annotated." Thirty-seven transcripts pertained to cellular processes, 49 were indicated in genetic information processing, 34 related to processing of environmental information, and 158 were implicated in cellular metabolism (8%, 10%, 8%, and 32%, respectively; Fig. 6a). The largest number of differentially expressed genes were related to the energy metabolism of the cell (Fig. 6a). Hierarchical clustering resulted in two clusters (Supporting Information Fig. S2), one containing the -Fe and the other the +Fe samples, revealing that Fe concentration rather than $p\text{CO}_2$ shaped the gene expression pattern in this experiment. Of the 1739 genes, 630 increased in

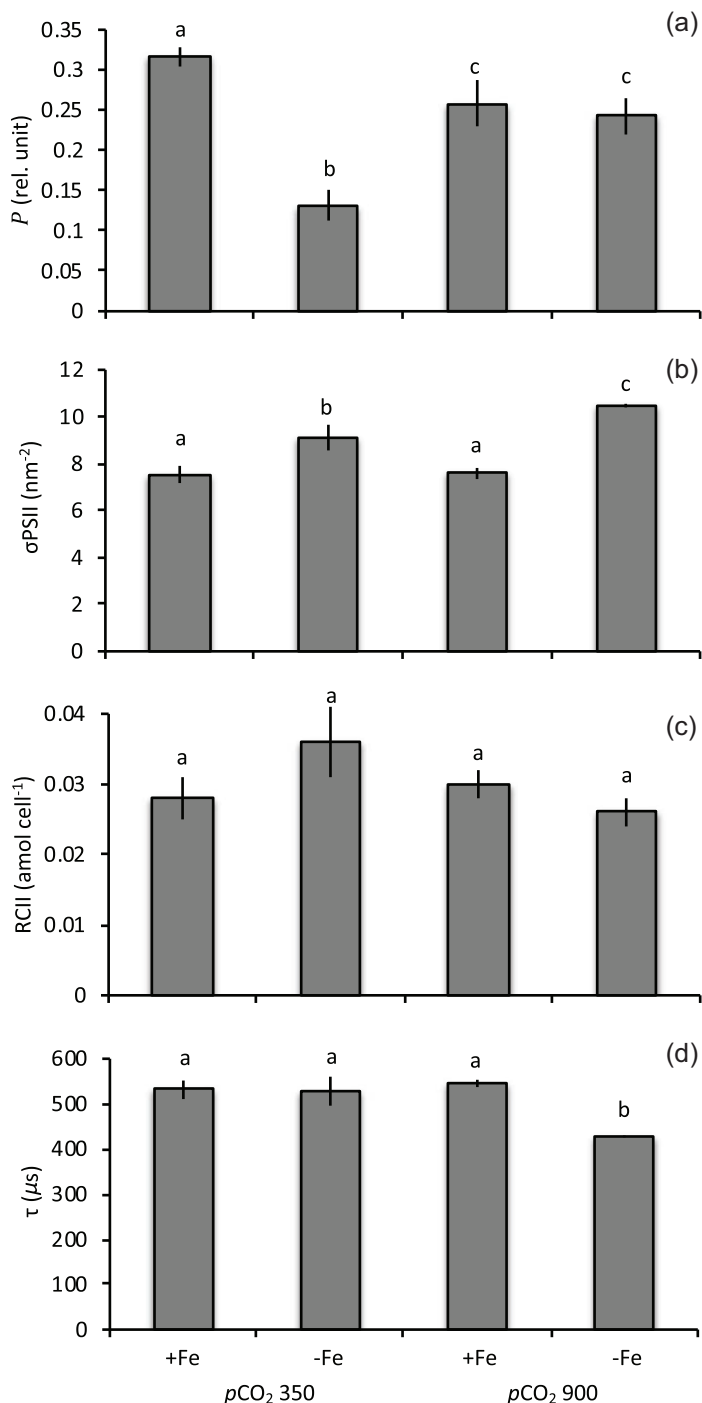


Fig. 4. Effects of iron (Fe) limitation and increased $p\text{CO}_2$ on the photo-physiological response of *P. antarctica* where **(a)** is the connectivity between photosystems, σPSII **(b)** represents the functional absorption cross section of PSII, RCII **(c)** represents the concentration of functional reaction centers for PSII, and τ **(d)** is the time constant for electron transport on the accelerator side of PSII. Cultures were grown under iron deplete (-Fe) and replete (+Fe) conditions and exposed to ambient (350 μatm) and elevated (900 μatm) $p\text{CO}_2$. Data shown represent mean \pm standard deviation ($n = 3$) of dark-adapted samples. Statistically significant differences (two-way ANOVA, $p < 0.05$) are denoted by varying small letters.

abundance while 1100 decreased under -Fe conditions (Fig. 6b; Supporting Information Data S1). Hierarchical clustering highlighted strong (Cluster I, +four fold changes over the +Fe; Supporting Information Data S1) and moderate increases (Cluster II, +one fold change over the +Fe; Supporting Information Data S1) while all of the genes, which decreased in abundance, belonged to the same cluster (Cluster I, Supporting Information Data S1). Genes encoding proteins involved in electron transport (respiratory and photosynthesis), nitrite/sulfite reduction and most Fuco-chlorophyll binding proteins were significantly lower under -Fe compared to +Fe conditions (Supporting Information Data S1). On the other hand, while no genes encoding ferric/ferrous ion transporters were annotated, genes encoding proteins involved in isoprenoid biosynthesis, catabolism of sugar compounds, triacylglycerol metabolism, cell cycle, protein degradation, locomotion/cell envelope were more highly expressed under -Fe conditions. The same was seen for genes annotated for plastocyanin, flavodoxin and several ferredoxin-dependent glutamate synthases. Finally, the expression of several genes involved in sugar metabolism was highly influenced by Fe availability, with some, like fructose-biphosphate aldolase and pyruvate kinase, showing a two-fold lower abundance under Fe limitation. Similarly, fructose-1,6-bisphosphatase class 1 and pyruvate carboxylase 1 and 2 transcripts increased almost two-fold from +Fe to -Fe (Supporting Information Data S1). Few CO_2 effects were evident as OA resulted in 45 and 34 differentially expressed transcripts in the +Fe and -Fe treatments, respectively (Fig. 6b). For +Fe and -Fe, only 11 and 12 transcripts, respectively, were annotated and did not show any pattern of the up- or downregulation of specific cellular processes (Supporting Information Data S1).

Discussion

Climate change will result in changes of various physical and chemical parameters including pH as well as Fe availability and speciation, which may differentially affect phytoplankton physiology. Fe limitation greatly reduced growth and POC production of *P. antarctica* and resulted in a significant change in cellular processes as evidenced by the large response in its transcriptome. Cellular concentrations of all TMs, not just Fe, were greatly reduced suggesting that Fe limitation may drive cells into secondary limitation by another TM (Cu, Co, Mn, or Zn). Conversely, OA did not significantly affect the majority of parameters measured. One major exception was the decreased production of HA-like substances under +Fe, which potentially changed TM chemistry and thus potentially the bioavailability of TMs.

Physiological responses of *P. antarctica* to Fe limitation trump those of OA

Low Fe conditions strongly inhibited the growth for *P. antarctica* (Fig. 1b). Our observations support previous studies, which reported a 40–50% decrease in growth rates for

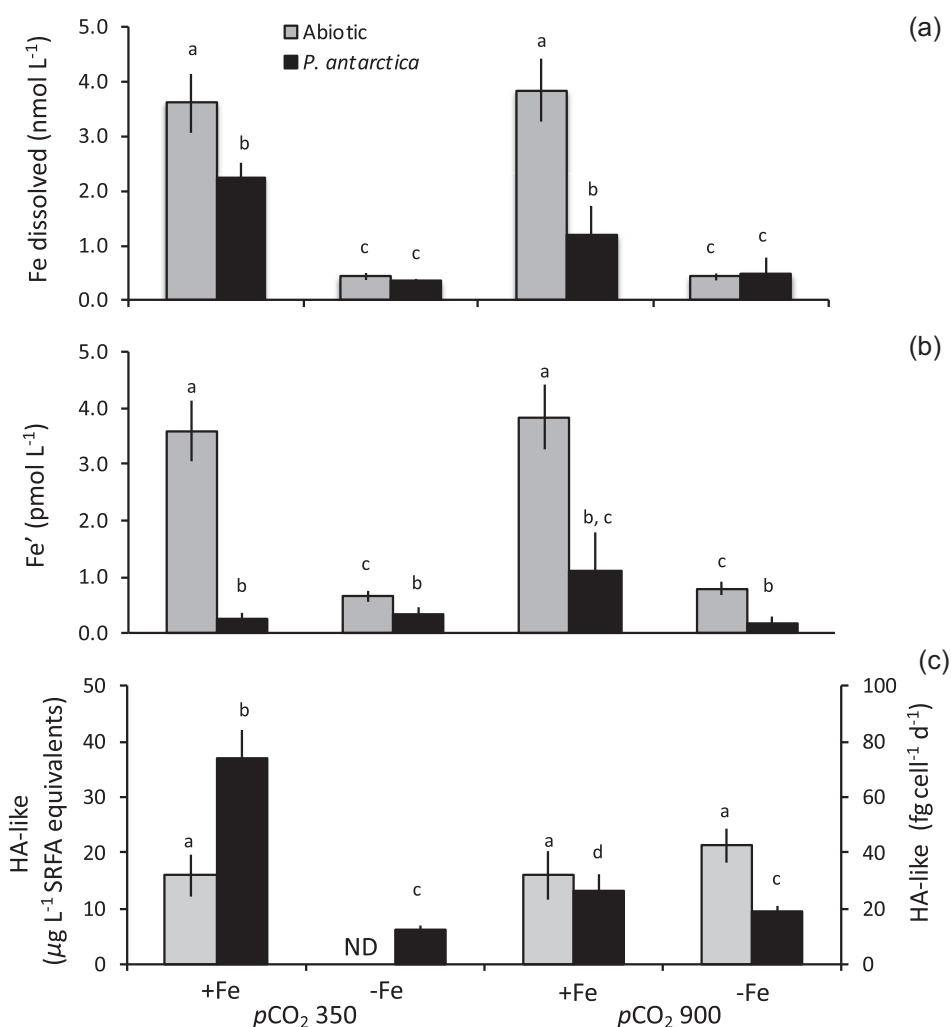


Fig. 5. Concentrations of total dissolved iron (dissolved Fe; **a**), dissolved inorganic iron (Fe'; **b**), and HA-like substances (**c**) determined at the end of the experiment. Concentrations were measured in seawater, in which either no (abiotic, gray bars) or *P. antarctica* cells (biotic, black bars) were present. Abiotic controls and cultures of *P. antarctica* were treated with either iron deplete (-Fe) or replete (+Fe) metal mix and exposed to ambient (350 μatm) and elevated (900 μatm) $p\text{CO}_2$. For the HA like, abiotic data represent the total concentration measured at the end of the experiment ($\mu\text{g L}^{-1}$ SRFA equivalents; see section), whereas the data for the cultures were normalized to biomass and incubation time ($\text{fg cell}^{-1} \text{d}^{-1}$). Data shown represent mean \pm standard deviation ($n = 3$). Statistical differences (two-way ANOVA, $p < 0.05$) are denoted by different small letters. "ND" denotes no data.

different strains of *P. antarctica* (Alderkamp et al. 2012; Strzepek et al. 2012) and other phytoplankton taxa (Allen et al. 2008; Nunn et al. 2013). Just like this study (Fig. 1a), the Fe-dependent reductions in growth rates were coupled to a significant loss in cell volume, in some cases by as much as 50% (Strzepek et al. 2012). This was further accompanied by a reduction in POC cell⁻¹ (Fig. 1c). Since transporters for Zn and possibly other TMs may already be operating at maximum efficiencies under low TM availability, the 28% reduction of cell volume observed during this study and the resulting 12% higher SA/V ratios likely reflect the organism's adaptation to the low Fe concentrations (Raven and Kubler 2002; Sunda 2012).

Since the concentration of RCII (amol cell^{-1}) was similar and aETR_{max} ($\text{e}^- \text{PSII}^{-1} \text{s}^{-1}$) were unchanged, (Fig. 4; Table 4),

Fe limitation inhibited the transport of energy equivalents downstream (i.e., PSI), resulting in smaller cell size and reduced POC production (Fig. 1d). Accordingly, genes encoding proteins involved in the synthesis of the main storage compound chrysolaminarin (β -1,3-glucan) in *P. antarctica* were down-regulated while others, involved in catabolism of various carbohydrates, were up-regulated (Supporting Information Data S1). Also, transcripts coding for fructose 1, 6 bisphosphatases, pyruvate carboxylases and a diacylglycerol O-acyltransferase increased under Fe deprivation (Supporting Information Data S1), indicating enhanced importance of other anabolic processes (such as gluconeogenesis, triacylglycerol synthesis). As a result of the lack in energy, storage compounds are catabolized or rearranged and then reused in respiration or protein synthesis in dark fixation.

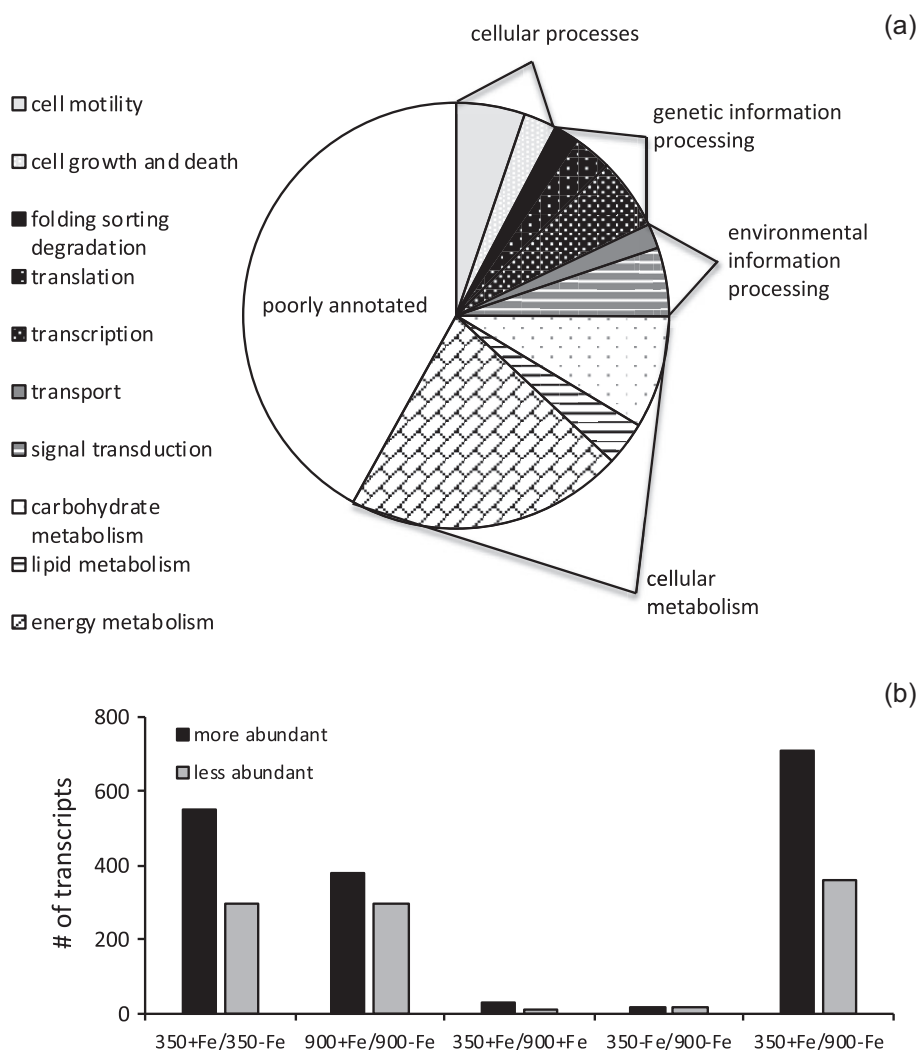


Fig. 6. Relative abundance of total differentially expressed gene transcripts (more and less abundant) annotated to various cellular processes comparing *P. antarctica* cells grown in Fe replete (+Fe) to limited (-Fe) media **(a)**. individual functional groups were grouped into cellular processes, genetic information processing, environmental information processing, and cellular metabolism (outside of pie). Absolute abundance (more or less abundant) of gene transcripts **(b)** comparing the various treatment conditions. Cultures were grown under Fe and +Fe conditions, exposed to ambient (350 = 350 μatm) and elevated (900 = 900 μatm) $p\text{CO}_2$.

Fe limitation likely also impacted other major cellular processes such as the nitrogen metabolism. As Fe is required for the enzymes ferredoxin-dependent nitrate and nitrite reductase, converting nitrate to nitrite in the former and nitrite to ammonium in the latter, Fe limitation can have a direct impact on the 'new nitrogen' supply of the cell (Morel et al. 1991; Milligan and Harrison 2000). In this study, C : N ratios for *P. antarctica* remained unchanged (Fig. 1e) and do not suggest N limitation. This is consistent with other studies, which have concluded that, with few exceptions, Fe limitation has a limited effect on the C : N ratio (Maldonado and Price 1996; Price 2005). There was, however, evidence for less abundant transcripts for nitrite reductase under -Fe conditions, suggesting a reduced capacity to assimilate nitrate. To compensate for this, amino acids were potentially reallocated/

recycled from proteins, as was evident due to the increase in transcripts coding for ubiquitin ligases and hydrolases in -Fe. Others have also described this pattern of protein recycling in Fe starved diatoms as one way to avoid N limitation (Allen et al. 2008; Nunn et al. 2013).

Stimulating effects of OA on phytoplankton physiology have been mainly linked to their carbon acquisition and photosynthetic carbon fixation, with elevated $p\text{CO}_2$ (lower pH) favoring species that benefit from higher diffusive CO_2 uptake (Petrou et al. 2016). No or even negative OA effects on growth and/or photosynthesis were previously reported for various SO diatoms (Riebesell et al. 1993; Boelen et al. 2011; Hoogstraten et al. 2012) and *P. antarctica* (Trimborn et al. 2013; Trimborn et al. 2017b). In this study, OA led to a slight increase in growth rates, but a decrease in POC per cell irrespective of Fe

availability. While this suggests that *P. antarctica* was able to adapt to OA, it did not result in net changes of cellular POC production. This effect was also evident when POC production rates were normalized to cell volume (Supporting Information Table S2) and suggests that in the future *P. antarctica*'s resilience to OA may provide it with a competitive advantage over other phytoplankton species, which are more sensitive to OA.

Fe limitation decreases cellular quotas of Fe and all other TMs

While cellular TM quotas for the -Fe are similar to those reported by others (see review in Twining and Baines 2013), concentrations in the +Fe were 5–10 fold higher than what has been reported for other experiments with *P. antarctica* (Strzepek et al. 2011; Strzepek et al. 2012). Cellular concentrations of TMs have been shown to vary greatly, not just between phytoplankton groups (Twining and Baines 2013), but also within a species (Ho et al. 2003; Sunda 2012). Also, TM quotas are affected by culture conditions and the methods of analysis used. As in our study, higher Fe:C quotas were reported when bulk filtration, an oxalate wash and subsequent analysis via ICPMS was used (King et al. 2012). In this study, we observed slightly higher cellular Zn:C than Fe:C than Twining and Baines (2013). This could be a result of the EDTA-free seawater media coupled to an oxalate wash. Zn may not be as efficiently removed from the cell surface as Fe. Another explanation could be that the much higher Zn concentrations typical of waters south of the polar front (Croot et al. 2011) could have resulted in the higher Zn:C ratios (Supporting Information Table S2) similar to other SO phytoplankton (Strzepek et al. 2011).

Sunda and Huntsman (1998b) introduced the idea of biodilution as an important process governing cellular TM concentrations. The cellular TM quota of an algal cell is a complicated interaction between different and sometimes competing uptake mechanisms (Sunda 2012) and the rate of biodilution by newly produced carbon. Thus, despite reduced POC production in -Fe cultures of *Thalassiosira pseudonana* (Sunda and Huntsman 2004) and *P. antarctica* (Lane et al. 2009), the uptake rates of other TMs, were similar, resulting in higher Zn:C and Cd:C ratios, respectively. In our study, however, concentrations of all TMs decreased under -Fe even though the dissolved concentrations of all TMs, except Fe, remained the same. This is in agreement with Annett et al. (2008) who observed that some temperate diatoms including *T. pseudonana* increased their Cu : C while others maintained or even decreased it.

TM acquisition in marine phytoplankton is complicated (Hudson and Morel 1990; Shaked et al. 2005) and despite many large scale environmental and laboratory experiments, the underlying mechanisms of TM uptake and utilization remain obscure (Morrissey and Bowler 2012). Whereas no genes for ferric or ferrous ion transporters could be found in

this study, a decreased abundance of genes coding for a Zn and mitochondrial metal ion transporter under -Fe conditions were observed. These findings support a reduction in the carbon normalized cellular TM quota when cells were Fe limited (Fig. 2a). A consequence of this might be that the availability of Fe limits the supply of other TMs, which, although sufficiently abundant in solution, may not be transported into the cell. This is evident by the significantly ($p < 0.001$) lower quotas of Zn, Cu, Mn, and Co in the -Fe treatments (Fig. 2b). Congruent to this study, Guo et al. (2012) also described a decrease of cellular Cu concentrations in *P. pouchetii* under -Fe conditions. In agreement with our findings, increases in the cellular quotas of other TMs, including Zn and Mn, were reported during a mesoscale Fe addition in the SO (Twining et al. 2004), demonstrating that a variety of cellular responses may happen when Fe is added. Similarly, the uptake of Cd in a coastal diatom was not regulated by external Cd concentrations, but rather concentrations of free ionic Mn and Zn Sunda and Huntsman (1998a). Whether the observed trends are related to the lack of energy due to the reduced efficiency of the light reaction or other enzymatic processes is not clear.

Even though OA effects on cell normalized Fe, Cu, Mn and Co quotas were observed in the +Fe treatments, except for Mn these trends disappeared when the values were normalized to carbon. This is in contrast to King et al. (2011), who found a positive correlation between elevated $p\text{CO}_2$ and cellular Fe : P, Fe : Zn, and Fe : Co ratios in the diatom *Attheya* sp. from the Bering Sea. The latter study, however, investigated effects at $p\text{CO}_2$ levels of 20, 370, and 670 ppm and it is possible that this trend would not hold at the $p\text{CO}_2$ of 950 μatm used in this study. The decrease of POC and maintenance of cellular TM stoichiometry, coupled to the observed increase in growth rates, suggests that under future OA conditions, the cellular TM demand of *P. antarctica* will not be affected. This is consistent with laboratory experiments that demonstrated that *P. antarctica* may be more resilient to OA (Trimborn et al. 2013, Trimborn et al. 2017b).

Iron limitation, not OA, drives the photophysiological response in *P. antarctica*

Thylakoid membranes and the associated photosynthesis are the dominant cellular sink for Fe (Raven et al. 1999), with Fe being critical in PSI, PSII and many other parts of the electron transport chain. Fe limitation caused critical restructuring of the thylakoid architecture, as seen by the decrease in the connectivity (P) between photosystems. This further accounted for the reduced photosynthetic efficiency (F_v/F_m) and consequently led to a less efficient transfer of electrons from PSII to PSI, observed here and by others (Strzepek et al. 2012; Petrou et al. 2014). Similar to van Leeuwe and Stefels (2007), under Fe limitation, *P. antarctica* decreased the concentrations of LH pigments and Fuco by 35% and 34%, respectively (Table 3). Moreover, transcriptomic analysis revealed 63 transcripts, annotated to LH centers, 85% of

which belonged to cluster I, or genes showing the greatest decrease in relative abundance. These include PSI reaction center subunit IV, chlorophyll *a-b* binding proteins (1B-21, 4, 7, L1818) and various Fuco-chlorophyll *a-c* binding proteins (A, B, C, D, E, and F). The lower concentrations of LH pigments were compensated by the increase of σ PSII by 25% (Fig. 4). Coupled to observations that the concentrations of functional reaction centers of PSII per cell (RCII) did not change (Fig. 4), our results suggest that *P. antarctica* adapts to low Fe conditions by increasing the size rather than the number of their photosynthetic units (Strzepak et al. 2011; Strzepak et al. 2012). *P. antarctica* further adapted to -Fe by switching to a more Fe-economical metabolism, substituting ferredoxin for flavodoxin, as seen in the three–six fold decrease and two–four fold increase in abundance of related genes, respectively (Supporting Information Data S1). Similarly, a two-fold increase of the relative abundance of plastocyanin a copper containing protein, which is similar in structure to the heme containing cytochrome c_6 , was observed. The latter was also found to decrease in abundance. As a consequence, *P. antarctica* was able to maintain similar cellular electron transport rates and light use efficiencies (I_k and α) when Fe limited (Supporting Information Table S4). Even though *P. antarctica* was able to maintain the same rate of aETR under Fe limitation, this energy did not result in an increase of POC production rates (Fig. 1). The latter observation suggests that alternate electron flow likely acted as a ‘safety valve’, which kept the primary quinone acceptor oxidized when excitation pressure on the electron chain was high. Similar observation was previously made for other Fe-limited phytoplankton (Schuback et al. 2015). Reduced abundance of transcripts for nitrite and sulfate reductases suggest that the excess energy, not turned into POC, was also not used in nitrogen or sulfur reduction. It is more plausible that the energy was dissipated by cyclic electron transport around PSII (Schuback et al. 2015; Heiden et al. 2016) or used in photorespiration (Beardall 1989). Heat dissipation in the xanthophyll cycle and nonphotochemical quenching, as evident by the increase in both the ratio of LP : LH pigments and NPQ in the -Fe treatments, also likely played an important role in protecting *P. antarctica* from excess energy (Fig. 3; Supporting Information Fig. S1). Like Alderkamp et al. (2012) and van Leeuwe and Stefels (2007), who reported a decrease of the de-epoxidation state in *P. antarctica* under -Fe, in this study Dt was reduced while Dd did not change, resulting in a four-fold lower DES under -Fe. Despite this reduction, the potential for photoprotection by NPQ was not affected as it was actually higher under -Fe than +Fe, confirming previous observations by Alderkamp et al. (2012).

Just like the other parameters assessed before, photophysiology was impacted to a much greater degree by Fe limitation than by OA. Trimborn et al. (2013, 2017a) observed no OA-dependent changes in the photophysiology or pigment composition of *P. antarctica* when compared to SO diatoms

grown under low and elevated irradiances. Similarly, OA also had no effect on the pigment composition and limited impact on the photosynthetic parameters measured in this study. Under Fe limitation, OA induced the highest σ PSII of any of the treatments (Fig. 4), leading to an increased LH efficiency, compensating thereby for the much lower amount of LH pigments per cell (Table 3). Similar to the response to Fe limitation under 350, higher aETR_{max} were also found at 900 in Fe-limited cells, but with much higher values (Table 4; Fig. 3). This indicates even stronger alternative electron cycling under these conditions (Schuback et al. 2015; Heiden et al. 2016). Dissipation of excess energy likely occurred through nonphotochemical quenching, as seen by the higher NPQ (Fig. 3c,d). In addition, the quickest τ of any of the treatments suggests the presence of alternative electron acceptors including Mehler reaction or photorespiration. The observed adjustments towards a more Fe-economical metabolism of *P. antarctica* under Fe limitation allowed this species to maintain the same rate of electron transport. However, the increase of aETR relative to carbon assimilation resulted in the need for alternative electron cycling in the -Fe, a trend observed even stronger under OA. Thus, while *P. antarctica* seems well equipped to adjust its photophysiology under Fe limitation to capture a similar amount of energy, this energy flow bottlenecks, is dissipated and not turned into biomass.

OA affects Fe chemistry indirectly

Not surprisingly the addition of Fe resulted in much higher Fe dissolved and Fe' concentrations but no change in the concentrations of HA-like substances in our abiotic controls (Fig. 5). In contrast, the presence of *Phaeocystis* cells resulted in the utilization of more of the dissolved Fe and Fe' in the +Fe compared to the -Fe. The fact that 92% and 51% of Fe' was taken up in the +Fe and -Fe treatments, respectively, while Fe dissolved decreased only by 39% and 25%, respectively, highlights increased utilization of more available forms of Fe by this species. This study confirms that actively growing cells of *P. antarctica* produce exopolymeric substances (HA-like), which are important in binding Fe and other TMs (Schoemann et al. 2001; Hassler et al. 2012). The significantly higher cellular concentrations of all TMs found in the +Fe treatment compared to the -Fe under 350 (Fig. 2) may be due to the increased production of metal binding polysaccharides. Several studies have reported a positive correlation between Fe uptake by phytoplankton and HA-like concentrations, suggesting a role of HA-like substances in Fe acquisition (Schoemann et al. 2001; Hassler et al. 2012; Trimborn et al. 2015). In our study, the increased HA-like production in the +Fe compared to the -Fe controls (Fig. 5) could have facilitated uptake of TMs in *P. antarctica*. Conversely HA-like production was lower in the -Fe, hence constraining TM uptake and amplifying the effects of Fe limitation.

One of the unknowns regarding climate change is how OA in the SO will impact TM chemistry and consequently primary

production and plankton species composition. OA may lead to changes in inorganic and organic TM complexation, and affect redox reactions and the precipitation of TMs (Hoffmann et al. 2012; Hutchins and Boyd 2016). Thus, changes to microbial communities with different TM quota and acquisition strategies, including changes in ligand production, and finally biological feedback mechanisms affecting all of the above, are likely (Hassler et al. 2011; Hassler et al. 2012). While Shi et al. (2010) reported reduced organically bound Fe uptake by diatoms under OA, Breitbarth et al. (2010) reported an increase in Fe bioavailability in a natural community OA experiment. This study shows that OA alone does not induce changes in TM chemistry since increased $p\text{CO}_2$ and the resulting drop in pH did not cause concentrations changes of Fe and HA-like substances in the abiotic controls (Fig. 5). Even though Fe replete *P. antarctica* cells produced less HA-like substances under OA (Fig. 5), this did not affect carbon normalized TM concentrations (Fig. 2). While the exact mechanisms responsible for this observation remain unclear, one reason may be that, due to a potential increase in bioavailability of TMs under OA, HA-like substances play a less important role.

Conclusions

P. antarctica, an ecologically important player in the phytoplankton community of the SO, routinely experiences Fe stress. Fe limitation resulted in dramatic changes in the physiology of *P. antarctica*, including a lower growth rate, reduction in cell size and Fe : C quota, and changes in photophysiology. In addition, Fe limitation, through yet unknown mechanisms, drastically lowered internal concentrations of other important TMs (Zn, Mn, Co, and Cu). While a cell may handle Fe limitation by restructuring their photosynthetic apparatus or nitrogen metabolism, as observed in this study, processes tightly coupled to the availability of other TMs may not be as easily substituted or switched. In other words, low Fe conditions may result in a cellular reduction of, and limitation by other TMs. Transcriptomic analysis revealed that Fe limitation had a much greater impact on this species than OA, resulting in a major rearrangement of cellular processes, especially carbohydrate, lipid and energy metabolism, which accounted for 33% of all differentially expressed transcripts. As *P. antarctica* is more tolerant to OA than other phytoplankton species such as diatoms (this study; Trimborn et al. 2013; Trimborn et al. 2017b), OA induced effects on the efficiency of the biological pump will likely arise from changes in species composition or changes in morphotypes (Feng et al. 2010; Hoppe et al. 2013; Trimborn et al. 2017a).

References

Abualhaija, M. M., and C. M. G. van den Berg. 2014. Chemical speciation of iron in seawater using catalytic cathodic stripping voltammetry with ligand competition against

- salicylaldehyde. *Mar. Chem.* **164**: 60–74. doi:[10.1016/j.marchem.2014.06.005](https://doi.org/10.1016/j.marchem.2014.06.005)
- Alderkamp, A. C. and others 2012. The effects of iron limitation on the photophysiology of *Phaeocystis Antarctica* (Prymnesiophyceae) and *Fragilariopsis cylindricus* (Bacillariophyceae) under dynamic irradiance. *J. Phycol.* **48**: 45–59. doi:[10.1111/j.1529-8817.2011.01098.x](https://doi.org/10.1111/j.1529-8817.2011.01098.x)
- Allen, A. E. and others 2008. Whole-cell response of the pennate diatom *Phaeodactylum tricorutum* to iron starvation. *Proc. Natl. Acad. Sci. USA* **105**: 10438–10443.
- Annett, A. L., S. Lapi, T. J. Ruth, and M. T. Maldonado. 2008. The effects of Cu and Fe availability on the growth and Cu : C ratios of marine diatoms. *Limnol. Oceanogr.* **53**: 2451–2461. doi:[10.4319/lo.2008.53.6.2451](https://doi.org/10.4319/lo.2008.53.6.2451)
- Arrigo, K. R. and others 1999. Phytoplankton community structure and the drawdown of nutrients and CO₂ in the Southern Ocean. *Science* **283**: 365–367. doi:[10.1126/science.283.5400.365](https://doi.org/10.1126/science.283.5400.365)
- Beardall, J. 1989. Photosynthesis and photorespiration in marine phytoplankton. *Aquat. Bot.* **34**: 105–130. doi:[10.1016/0304-3770\(89\)90052-1](https://doi.org/10.1016/0304-3770(89)90052-1)
- Behrenfeld, M. J., and A. J. Milligan. 2013. Photophysiological expressions of iron stress in phytoplankton. *Ann. Rev. Mar. Sci.* **5**: 217–246. doi:[10.1146/annurev-marine-121211-172356](https://doi.org/10.1146/annurev-marine-121211-172356)
- Bertrand, E. M. and others 2007. Vitamin B-12 and iron colimitation of phytoplankton growth in the Ross Sea. *Limnol. Oceanogr.* **52**: 1079–1093. doi:[10.4319/lo.2007.52.3.1079](https://doi.org/10.4319/lo.2007.52.3.1079)
- Boelen, P., W. H. V. de Poll, H. J. van der Strate, I. A. Neven, J. Beardall, and A. G. J. Buma. 2011. Neither elevated nor reduced CO₂ affects the photophysiological performance of the marine Antarctic diatom *Chaetoceros brevis*. *J. Exp. Mar. Biol. Ecol.* **406**: 38–45. doi:[10.1016/j.jembe.2011.06.012](https://doi.org/10.1016/j.jembe.2011.06.012)
- Bolger, A. M., M. Lohse, and B. Usadel. 2014. Trimmomatic: A flexible trimmer for Illumina sequence data. *Bioinformatics* **30**: 2114–2120. doi:[10.1093/bioinformatics/btu170](https://doi.org/10.1093/bioinformatics/btu170)
- Boyd, P. W., and M. J. Ellwood. 2010. The biogeochemical cycle of iron in the ocean. *Nat. Geosci.* **3**: 675–682. doi:[10.1038/ngeo964](https://doi.org/10.1038/ngeo964)
- Boyd, P. W. and others 2005. The evolution and termination of an iron-induced mesoscale bloom in the northeast subarctic Pacific. *Limnol. Oceanogr.* **50**: 1872–1886. doi:[10.4319/lo.2005.50.6.1872](https://doi.org/10.4319/lo.2005.50.6.1872)
- Boye, M., C. M. G. van den Berg, J. T. M. de Jong, H. Leach, P. Croot, and H. J. W. de Baar. 2001. Organic complexation of iron in the Southern Ocean. *Deep-Sea Res. Part I-Oceanogr. Res. Pap.* **48**: 1477–1497. doi:[10.1016/S0967-0637\(00\)00099-6](https://doi.org/10.1016/S0967-0637(00)00099-6)
- Breitbarth, E. and others 2010. Ocean acidification affects iron speciation during a coastal seawater mesocosm experiment. *Biogeosciences* **7**: 1065–1073. doi:[10.5194/bg-7-1065-2010](https://doi.org/10.5194/bg-7-1065-2010)
- Brewer, P. G., A. L. Bradshaw, and R. T. Williams. 1986. Measurements of total carbon dioxide and alkalinity in the North Atlantic Ocean in 1981, p. 348–370. *In* J. R. Trabalka and D. E. Reichle [eds.], *The changing carbon cycle, a global analysis*. Springer.

- Buesseler, K. O. 1998. The decoupling of production and particulate export in the surface ocean. *Global Biogeochem. Cycle* **12**: 297–310. doi:[10.1029/97GB03366](https://doi.org/10.1029/97GB03366)
- Croot, P. L., and M. Johansson. 2000. Determination of iron speciation by cathodic stripping voltammetry in seawater using the competing ligand 2-(2-thiazolylazo)-p-cresol (TAC). *Electroanalysis* **12**: 565–576. doi:[10.1002/\(SICI\)1521-4109\(200005\)12:8<565:AID-ELAN565>3.0.CO;2-L](https://doi.org/10.1002/(SICI)1521-4109(200005)12:8<565:AID-ELAN565>3.0.CO;2-L)
- Croot, P. L., O. Baars, and P. Streu. 2011. The distribution of dissolved zinc in the Atlantic sector of the Southern Ocean. *Deep-Sea Res. Part II-Top. Stud. Oceanogr.* **58**: 2707–2719. doi:[10.1016/j.dsr2.2010.10.041](https://doi.org/10.1016/j.dsr2.2010.10.041)
- Cutter, G. and others 2017. Sampling and sample-handling protocols for GEOTRACES cruises. GEOTRACES International Project Office, p. 139. doi:[10.1145/3075300](https://doi.org/10.1145/3075300)
- Cvetkovic, A. and others 2010. Microbial metalloproteomes are largely uncharacterized. *Nature* **466**: 779–782. doi:[10.1038/nature09265](https://doi.org/10.1038/nature09265)
- de Baar, H. J. W. and others 2005. Synthesis of iron fertilization experiments: From the iron age in the age of enlightenment. *J. Geophys. Res. Oceans* **110**: 1–24. doi:[10.1029/2004JC002601](https://doi.org/10.1029/2004JC002601)
- Dickson, A. G., and F. J. Millero. 1987. A comparison of the equilibrium-constants for the dissociation of carbonic-acid in seawater media. *Deep-Sea Res. Part A-Oceanogr. Res. Pap.* **34**: 1733–1743. doi:[10.1016/0198-0149\(87\)90021-5](https://doi.org/10.1016/0198-0149(87)90021-5)
- DiTullio, G. R., N. Garcia, S. F. Riseman, and P. N. Sedwick. 2007. Effects of iron concentration on pigment composition in *Phaeocystis Antarctica* grown at low irradiance. *Biogeochemistry* **83**: 71–81. doi:[10.1007/s10533-007-9080-8](https://doi.org/10.1007/s10533-007-9080-8)
- Feng, Y. and others 2010. Interactive effects of iron, irradiance and CO₂ on Ross Sea phytoplankton. *Deep-Sea Res. Part I-Oceanogr. Res. Pap.* **57**: 368–383. doi:[10.1016/j.dsr.2009.10.013](https://doi.org/10.1016/j.dsr.2009.10.013)
- Fishwick, M. P. and others 2014. The impact of changing surface ocean conditions on the dissolution of aerosol iron. *Global Biogeochem. Cycle* **28**: 1235–1250. doi:[10.1002/2014GB004921](https://doi.org/10.1002/2014GB004921)
- Genty, B., J. M. Briantais, and N. R. Baker. 1989. The relationship between the quantum yield of photosynthetic electron-transport and quenching of chlorophyll fluorescence. *Biochim. Biophys. Acta* **990**: 87–92. doi:[10.1016/S0304-4165\(89\)80016-9](https://doi.org/10.1016/S0304-4165(89)80016-9)
- Gerringa, L. J. A., P. M. J. Herman, and T. C. W. Poortvliet. 1995. Comparison of the linear Vandenberg Ruzic transformation and a nonlinear fit of the Langmuir isotherm applied to Cu speciation data in the estuarine environment. *Mar. Chem.* **48**: 131–142. doi:[10.1016/0304-4203\(94\)00041-B](https://doi.org/10.1016/0304-4203(94)00041-B)
- Gerringa, L. J. A., H. J. W. de Baar, and K. R. Timmermans. 2000. A comparison of iron limitation of phytoplankton in natural oceanic waters and laboratory media conditioned with EDTA. *Mar. Chem.* **68**: 335–346. doi:[10.1016/S0304-4203\(99\)00092-4](https://doi.org/10.1016/S0304-4203(99)00092-4)
- Grabherr, M. G. and others 2011. Full-length transcriptome assembly from RNA-Seq data without a reference genome. *Nat. Biotechnol.* **29**: 644–U130. doi:[10.1038/nbt.1883](https://doi.org/10.1038/nbt.1883)
- Gran, G. 1952. Determination of the equivalence point in potentiometric titrations-part II. *Analyst* **77**: 661–671. doi:[10.1039/an9527700661](https://doi.org/10.1039/an9527700661)
- Guillard, R. R., and J. H. Ryther. 1962. Studies of marine planktonic diatoms. 1. *Cyclotella nana* (Hustedt) and *Detonula confervacea* (Cleve) gran. *Can. J. Microbiol.* **8**: 229–239. doi:[10.1139/m62-029](https://doi.org/10.1139/m62-029)
- Guo, J., et al. 2012. The effects of iron and copper availability on the copper stoichiometry of marine phytoplankton. *J. Phycol.* **48**: 312–325.
- Hassler, C. S., and V. Schoemann. 2009. Discriminating between intra- and extracellular metals using chemical extractions: An update on the case of iron. *Limnol. Oceanogr.: Methods* **7**: 479–489. doi:[10.4319/lom.2009.7.479](https://doi.org/10.4319/lom.2009.7.479)
- Hassler, C. S., V. Schoemann, C. M. Nichols, E. C. V. Butler, and P. W. Boyd. 2011. Saccharides enhance iron bioavailability to Southern Ocean phytoplankton. *Proc. Natl. Acad. Sci. USA* **108**: 1076–1081. doi:[10.1073/pnas.1010963108](https://doi.org/10.1073/pnas.1010963108)
- Hassler, C. S., V. Schoemann, M. Boye, A. Tagliabue, M. Rozmarynowycz, and R. M. L. McKay. 2012. Iron bioavailability in the Southern Ocean p. 1–63. *In* R. N. Gibson, R. J. A. Atkinson, J. D. M. Gordon and R. N. Hughes [eds.], *Oceanography and marine biology: An annual review*, V. **50**. CRC Press.
- Hathorne, E. C., B. Haley, T. Stichel, P. Grasse, M. Zieringer, and M. Frank. 2012. Online preconcentration ICP-MS analysis of rare earth elements in seawater. *Geochim. Geophys. Geosyst.* **13**: 12. doi:[10.1029/2011GC003907](https://doi.org/10.1029/2011GC003907)
- Heiden, J. P., K. Bischof, and S. Trimborn. 2016. Light intensity modulates the response of two Antarctic diatom species to ocean acidification. *Front. Mar. Sci.* **3**: 260. doi:[10.3389/fmars.2016.00260](https://doi.org/10.3389/fmars.2016.00260)
- Ho, T. Y. and others 2003. The elemental composition of some marine phytoplankton. *J. Phycol.* **39**: 1145–1159. doi:[10.1111/j.0022-3646.2003.03-090.x](https://doi.org/10.1111/j.0022-3646.2003.03-090.x)
- Hoffmann, L. J., E. Breitbarth, P. W. Boyd, and K. A. Hunter. 2012. Influence of ocean warming and acidification on trace metal biogeochemistry. *Mar. Ecol. Prog. Ser.* **470**: 191–205. doi:[10.3354/meps10082](https://doi.org/10.3354/meps10082)
- Hoogstraten, A., K. R. Timmermans, and H. J. W. de Baar. 2012. Morphological and physiological effects in *Proboscia alata* (Bacillariophyceae) grown under different light and CO₂ conditions of the modern Southern Ocean. *J. Phycol.* **48**: 559–568. doi:[10.1111/j.1529-8817.2012.01148.x](https://doi.org/10.1111/j.1529-8817.2012.01148.x)
- Hoppe, C. J. M., C. S. Hassler, C. D. Payne, P. D. Tortell, B. Rost, and S. Trimborn. 2013. Iron limitation modulates ocean acidification effects on Southern Ocean phytoplankton communities. *PLoS One* **8**: 9. doi:[10.1371/journal.pone.0079890](https://doi.org/10.1371/journal.pone.0079890)
- Hoppe, C. J. M., L. M. Holtz, S. Trimborn, and B. Rost. 2015. Ocean acidification decreases the light-use efficiency in an

- Antarctic diatom under dynamic but not constant light. *New Phytol.* **207**: 159–171. doi:[10.1111/nph.13334](https://doi.org/10.1111/nph.13334)
- Hudson, R. J. M., and F. M. M. Morel. 1990. Iron transport in marine phytoplankton—kinetics of cellular and medium coordination reactions. *Limnol. Oceanogr.* **35**: 1002–1020. doi:[10.4319/lo.1990.35.5.1002](https://doi.org/10.4319/lo.1990.35.5.1002)
- Huot, Y., and M. Babin. 2010. Overview of fluorescence protocols: Theory, basic concepts, and practice. *Chlorophyll a fluorescence in aquatic sciences: Methods and applications*. Springer.
- Hutchins, D. A., A. E. Witter, A. Butler, and G. W. Luther. 1999. Competition among marine phytoplankton for different chelated iron species. *Nature* **400**: 858–861. doi:[10.1038/23680](https://doi.org/10.1038/23680)
- Hutchins, D. A., and P. W. Boyd. 2016. Marine phytoplankton and the changing ocean iron cycle. *Nat. Clim. Change* **6**: 1072–1079. doi:[10.1038/nclimate3147](https://doi.org/10.1038/nclimate3147)
- IPCC. 2014. Climate change 2014: Synthesis report. Contribution of Working Groups I, II and III to the Fifth Assessment Report of the Intergovernmental Panel on Climate Change. In R. K. Pachauri and L. A. Meyer [eds.]. IPCC.
- King, A. L., S. A. Sanudo-Wilhelmy, K. Leblanc, D. A. Hutchins, and F. X. Fu. 2011. CO₂ and vitamin B-12 interactions determine bioactive trace metal requirements of a subarctic Pacific diatom. *ISME J.* **5**: 1388–1396. doi:[10.1038/ismej.2010.211](https://doi.org/10.1038/ismej.2010.211)
- King, A. L. and others 2012. A comparison of biogenic iron quotas during a diatom spring bloom using multiple approaches. *Biogeosciences* **9**: 667–687. doi:[10.5194/bg-9-667-2012](https://doi.org/10.5194/bg-9-667-2012)
- Koch, F., M. A. Marcoval, C. Panzeca, K. W. Bruland, S. A. Sanudo-Wilhelmy, and C. J. Gobler. 2011. The effect of vitamin B-12 on phytoplankton growth and community structure in the Gulf of Alaska. *Limnol. Oceanogr.* **56**: 1023–1034. doi:[10.4319/lo.2011.56.3.1023](https://doi.org/10.4319/lo.2011.56.3.1023)
- Kolber, Z. S., O. Prasil, and P. G. Falkowski. 1998. Measurements of variable chlorophyll fluorescence using fast repetition rate techniques: Defining methodology and experimental protocols. *Biochim. Biophys. Acta* **1367**: 88–106. doi:[10.1016/S0005-2728\(98\)00135-2](https://doi.org/10.1016/S0005-2728(98)00135-2)
- Kuma, K., J. Nishioka, and K. Matsunaga. 1996. Controls on iron(III) hydroxide solubility in seawater: The influence of pH and natural organic chelators. *Limnol. Oceanogr.* **41**: 396–407. doi:[10.4319/lo.1996.41.3.0396](https://doi.org/10.4319/lo.1996.41.3.0396)
- Laglera, L. M., G. Battaglia, and C. M. G. van den Berg. 2007. Determination of humic substances in natural waters by cathodic stripping voltammetry of their complexes with iron. *Anal. Chim. Acta* **599**: 58–66. doi:[10.1016/j.aca.2007.07.059](https://doi.org/10.1016/j.aca.2007.07.059)
- Laglera, L. M., and C. M. G. van den Berg. 2009. Evidence for geochemical control of iron by humic substances in seawater. *Limnol. Oceanogr.* **54**: 610–619. doi:[10.4319/lo.2009.54.2.0610](https://doi.org/10.4319/lo.2009.54.2.0610)
- Landschutzer, P. and others 2015. The reinvigoration of the Southern Ocean carbon sink. *Science* **349**: 1221–1224. doi:[10.1126/science.aab2620](https://doi.org/10.1126/science.aab2620)
- Lane, E. S., D. M. Semeniuk, R. F. Strzepek, J. T. Cullen, and M. T. Maldonado. 2009. Effects of iron limitation on intracellular cadmium of cultured phytoplankton: Implications for surface dissolved cadmium to phosphate ratios. *Mar. Chem.* **115**: 155–162. doi:[10.1016/j.marchem.2009.07.008](https://doi.org/10.1016/j.marchem.2009.07.008)
- Langmead, B., C. Trapnell, M. Pop, and S. L. Salzberg. 2009. Ultrafast and memory-efficient alignment of short DNA sequences to the human genome. *Genome Biol.* **10**: 10. doi:[10.1186/gb-2009-10-3-r25](https://doi.org/10.1186/gb-2009-10-3-r25)
- Lelandais, G. and others 2016. *Ostreococcus tauri* is a new model green alga for studying iron metabolism in eukaryotic phytoplankton. *BMC Genomics* **17**: 1–23. doi:[10.1186/s12864-016-2666-6](https://doi.org/10.1186/s12864-016-2666-6)
- Li, B., and C. N. Dewey. 2011. RSEM: Accurate transcript quantification from RNA-Seq data with or without a reference genome. *Bmc Bioinformatics* **12**: 323. doi:[10.1186/1471-2105-12-323](https://doi.org/10.1186/1471-2105-12-323)
- Liu, X. W., and F. J. Millero. 2002. The solubility of iron in seawater. *Mar. Chem.* **77**: 43–54. doi:[10.1016/S0304-4203\(01\)00074-3](https://doi.org/10.1016/S0304-4203(01)00074-3)
- Lumpkin, R., and K. Speer. 2007. Global ocean meridional overturning. *J. Phys. Oceanogr.* **37**: 2550–2562. doi:[10.1175/JPO3130.1](https://doi.org/10.1175/JPO3130.1)
- Maldonado, M. T., and N. M. Price. 1996. Influence of N substrate on Fe requirements of marine centric diatoms. *Mar. Ecol. Prog. Ser.* **141**: 161–172. doi:[10.3354/meps141161](https://doi.org/10.3354/meps141161)
- Maldonado, M. T., R. F. Strzepek, S. Sander, and P. W. Boyd. 2005. Acquisition of iron bound to strong organic complexes, with different Fe binding groups and photochemical reactivities, by plankton communities in Fe-limited subantarctic waters. *Global Biogeochem. Cycle* **19**: 15. doi:[10.1029/2005GB002481](https://doi.org/10.1029/2005GB002481)
- Martin, J. H., and S. E. Fitzwater. 1988. Iron deficiency limits phytoplankton growth in the Northeast Pacific subarctic. *Nature* **331**: 341–343. doi:[10.1038/331341a0](https://doi.org/10.1038/331341a0)
- Martin, J. H., R. M. Gordon, and S. E. Fitzwater. 1990. Iron in Antarctic waters. *Nature* **345**: 156–158. doi:[10.1038/345156a0](https://doi.org/10.1038/345156a0)
- McQuaid, J. B. and others 2018. Carbonate-sensitive phyto-transferrin controls high-affinity iron uptake in diatoms. *Nature* **555**: 534–537. doi:[10.1038/nature25982](https://doi.org/10.1038/nature25982)
- Mehrbach, C., C. H. Culbertson, J. E. Hawley, and R. M. Pytkowicz. 1973. Measurements of the apparent dissociation constants of carbonic acid in seawater at atmospheric pressure. *Limnol. Oceanogr.* **18**: 897–907. doi:[10.4319/lo.1973.18.6.0897](https://doi.org/10.4319/lo.1973.18.6.0897)
- Millero, F. J., R. Woosley, B. Ditrolio, and J. Waters. 2009. Effect of ocean acidification on the speciation of metals in seawater. *Oceanography* **22**: 72–85. doi:[10.5670/oceanog.2009.98](https://doi.org/10.5670/oceanog.2009.98)
- Milligan, A. J., and P. J. Harrison. 2000. Effects of non-steady-state iron limitation on nitrogen assimilatory enzymes in the marine diatom *Thalassiosira weissflogii* (Bacillariophyceae). *J. Phycol.* **36**: 78–86. doi:[10.1046/j.1529-8817.2000.99013.x](https://doi.org/10.1046/j.1529-8817.2000.99013.x)
- Morel, F. M. M., R. J. M. Hudson, and N. M. Price. 1991. Limitation of productivity by trace-metals in the sea. *Limnol. Oceanogr.* **36**: 1742–1755. doi:[10.4319/lo.1991.36.8.1742](https://doi.org/10.4319/lo.1991.36.8.1742)

- Morrissey, J., and C. Bowler. 2012. Iron utilization in marine cyanobacteria and eukaryotic algae. *Front. Microbiol.* **3**: 13. doi:[10.3389/fmicb.2012.00043](https://doi.org/10.3389/fmicb.2012.00043)
- Nunn, B. L. and others 2013. Diatom proteomics reveals unique acclimation strategies to mitigate Fe limitation. *PLoS One*: 8: e75653. doi:[10.1371/journal.pone.0075653](https://doi.org/10.1371/journal.pone.0075653)
- Oxborough, K., C. M. Moore, D. J. Suggett, T. Lawson, H. G. Chan, and R. J. Geider. 2012. Direct estimation of functional PSII reaction center concentration and PSII electron flux on a volume basis: A new approach to the analysis of fast repetition rate fluorometry (FRRf) data. *Limnol. Oceanogr.: Methods* **10**: 142–154. doi:[10.4319/lom.2012.10.142](https://doi.org/10.4319/lom.2012.10.142)
- Petrou, K., S. Trimborn, B. Rost, P. J. Ralph, and C. S. Hassler. 2014. The impact of iron limitation on the physiology of the Antarctic diatom *Chaetoceros simplex*. *Mar. Biol.* **161**: 925–937. doi:[10.1007/s00227-014-2392-z](https://doi.org/10.1007/s00227-014-2392-z)
- Petrou, K. and others 2016. Southern Ocean phytoplankton physiology in a changing climate. *J. Plant Physiol.* **203**: 135–150. doi:[10.1016/j.jplph.2016.05.004](https://doi.org/10.1016/j.jplph.2016.05.004)
- Pierrot, D., E. Lewis, and D. W. R. Wallace. 2006. MS excel program developed for CO₂ system calculations. ORNL/CDIAC-105. U.S. Department of Energy. doi:[10.1074/jbc.M606015200](https://doi.org/10.1074/jbc.M606015200)
- Price, N. M. 2005. The elemental stoichiometry and composition of an iron-limited diatom. *Limnol. Oceanogr.* **50**: 1159–1171. doi:[10.4319/lo.2005.50.4.1159](https://doi.org/10.4319/lo.2005.50.4.1159)
- Ralph, P. J., and R. Gademann. 2005. Rapid light curves: A powerful tool to assess photosynthetic activity. *Aquat. Bot.* **82**: 222–237. doi:[10.1016/j.aquabot.2005.02.006](https://doi.org/10.1016/j.aquabot.2005.02.006)
- Raven, J. A., M. C. W. Evans, and R. E. Korb. 1999. The role of trace metals in photosynthetic electron transport in O₂-evolving organisms. *Photosynth. Res.* **60**: 111–149. doi:[10.1023/A:1006282714942](https://doi.org/10.1023/A:1006282714942)
- Raven, J. A., and J. E. Kubler. 2002. New light on the scaling of metabolic rate with the size of algae. *J. Phycol.* **38**: 11–16. doi:[10.1046/j.1529-8817.2002.01125.x](https://doi.org/10.1046/j.1529-8817.2002.01125.x)
- Riebesell, U., D. A. Wolfgladow, and V. Smetacek. 1993. Carbon-dioxide limitation of marine-phytoplankton growth-rates. *Nature* **361**: 249–251. doi:[10.1038/361249a0](https://doi.org/10.1038/361249a0)
- Robinson, M. D. et al. 2010. edgeR: a Bioconductor package for differential expression analysis of digital gene expression data. *Bioinformatics* **26**: 139–140.
- Rue, E. L., and K. W. Bruland. 1995. Complexation of iron(III) by natural organic-ligands in the central North Pacific as determined by a new competitive ligand equilibrium adsorptive cathodic stripping voltammetric method. *Mar. Chem.* **50**: 117–138. doi:[10.1016/0304-4203\(95\)00031-L](https://doi.org/10.1016/0304-4203(95)00031-L)
- Sabine, C. L. and others 2004. The oceanic sink for anthropogenic CO₂. *Science* **305**: 367–371. doi:[10.1126/science.1097403](https://doi.org/10.1126/science.1097403)
- Schoemann, V., R. Wollast, L. Chou, and C. Lancelot. 2001. Effects of photosynthesis on the accumulation of Mn and Fe by *Phaeocystis* colonies. *Limnol. Oceanogr.* **46**: 1065–1076. doi:[10.4319/lo.2001.46.5.1065](https://doi.org/10.4319/lo.2001.46.5.1065)
- Schuback, N., C. Schallenberg, C. Duckham, M. T. Maldonado, and P. D. Tortell. 2015. Interacting effects of light and iron availability on the coupling of photosynthetic electron transport and CO₂-assimilation in marine phytoplankton. *PLoS One* **10**: e0133235. doi:[10.1371/journal.pone.0133235](https://doi.org/10.1371/journal.pone.0133235)
- Shaked, Y., A. B. Kustka, and F. M. M. Morel. 2005. A general kinetic model for iron acquisition by eukaryotic phytoplankton. *Limnol. Oceanogr.* **50**: 872–882. doi:[10.4319/lo.2005.50.3.0872](https://doi.org/10.4319/lo.2005.50.3.0872)
- Shi, D. L., Y. Xu, B. M. Hopkinson, and F. M. M. Morel. 2010. Effect of ocean acidification on iron availability to marine phytoplankton. *Science* **327**: 676–679. doi:[10.1126/science.1183517](https://doi.org/10.1126/science.1183517)
- Smith, W. O., J. Marra, M. R. Hiscock, and R. T. Barber. 2000. The seasonal cycle of phytoplankton biomass and primary productivity in the Ross Sea, Antarctica. *Deep-Sea Res. Part II-Top. Stud. Oceanogr.* **47**: 3119–3140. doi:[10.1016/S0967-0645\(00\)00061-8](https://doi.org/10.1016/S0967-0645(00)00061-8)
- Stoll, M. H. C., K. Bakker, G. H. Nobbe, and R. R. Haese. 2001. Continuous-flow analysis of dissolved inorganic carbon content in seawater. *Anal. Chem.* **73**: 4111–4116. doi:[10.1021/ac010303r](https://doi.org/10.1021/ac010303r)
- Strzepek, R. F., M. T. Maldonado, K. A. Hunter, R. D. Frew, and P. W. Boyd. 2011. Adaptive strategies by Southern Ocean phytoplankton to lessen iron limitation: Uptake of organically complexed iron and reduced cellular iron requirements. *Limnol. Oceanogr.* **56**: 1983–2002. doi:[10.4319/lo.2011.56.6.1983](https://doi.org/10.4319/lo.2011.56.6.1983)
- Strzepek, R. F., K. A. Hunter, R. D. Frew, P. J. Harrison, and P. W. Boyd. 2012. Iron-light interactions differ in Southern Ocean phytoplankton. *Limnol. Oceanogr.* **57**: 1182–1200. doi:[10.4319/lo.2012.57.4.1182](https://doi.org/10.4319/lo.2012.57.4.1182)
- Suggett, D. J., C. M. Moore, A. E. Hickman, and R. J. Geider. 2009. Interpretation of fast repetition rate (FRR) fluorescence: Signatures of phytoplankton community structure versus physiological state. *Mar. Ecol. Prog. Ser.* **376**: 1–19. doi:[10.3354/meps07830](https://doi.org/10.3354/meps07830)
- Sunda, W. G. 2012. Feedback interactions between trace metal nutrients and phytoplankton in the ocean. *Front. Microbiol.* **3**: 1–22. doi:[10.3389/fmicb.2012.00204](https://doi.org/10.3389/fmicb.2012.00204)
- Sunda, W. G., and S. A. Huntsman. 1998a. Interactions among Cu²⁺, Zn²⁺, and Mn²⁺ in controlling cellular Mn, Zn, and growth rate in the coastal alga *Chlamydomonas*. *Limnol. Oceanogr.* **43**: 1055–1064. doi:[10.4319/lo.1998.43.6.1055](https://doi.org/10.4319/lo.1998.43.6.1055)
- Sunda, W. G., and S. A. Huntsman. 1998b. Processes regulating cellular metal accumulation and physiological effects: Phytoplankton as model systems. *Sci. Total Environ.* **219**: 165–181. doi:[10.1016/S0048-9697\(98\)00226-5](https://doi.org/10.1016/S0048-9697(98)00226-5)
- Sunda, W. G., and S. A. Huntsman. 2004. Relationships among photoperiod, carbon fixation, growth, chlorophyll a, and cellular iron and zinc in a coastal diatom. *Limnol. Oceanogr.* **49**: 1742–1753. doi:[10.4319/lo.2004.49.5.1742](https://doi.org/10.4319/lo.2004.49.5.1742)
- Trimborn, S., T. Brenneis, E. Sweet, and B. Rost. 2013. Sensitivity of Antarctic phytoplankton species to ocean acidification:

- Growth, carbon acquisition, and species interaction. *Limnol. Oceanogr.* **58**: 997–1007. doi:[10.4319/lo.2013.58.3.0997](https://doi.org/10.4319/lo.2013.58.3.0997)
- Trimborn, S., C. J. M. Hoppe, B. B. Taylor, A. Bracher, and C. Hassler. 2015. Physiological characteristics of open ocean and coastal phytoplankton communities of Western Antarctic peninsula and Drake Passage waters. *Deep-Sea Res. Part I-Oceanogr. Res. Pap.* **98**: 115–124. doi:[10.1016/j.dsr.2014.12.010](https://doi.org/10.1016/j.dsr.2014.12.010)
- Trimborn, S., S. Thoms, T. Brenneis, J. P. Heiden, S. Beszteri, and K. Bischof. 2017a. Two Southern Ocean diatoms are more sensitive to ocean acidification and changes in irradiance than the prymnesiophyte *Phaeocystis Antarctica*. *Physiol. Plant.* **160**: 155–170. doi:[10.1111/ppl.12539](https://doi.org/10.1111/ppl.12539)
- Trimborn, S. and others 2017b. Iron sources alter the response of Southern Ocean phytoplankton to ocean acidification. *Mar. Ecol. Prog. Ser.* **578**: 35–50. doi:[10.3354/meps12250](https://doi.org/10.3354/meps12250)
- Twining, B. S., S. B. Baines, and N. S. Fisher. 2004. Element stoichiometries of individual plankton cells collected during the Southern Ocean iron experiment (SOFEX). *Limnol. Oceanogr.* **49**: 2115–2128. doi:[10.4319/lo.2004.49.6.2115](https://doi.org/10.4319/lo.2004.49.6.2115)
- Twining, B. S., and S. B. Baines. 2013. The trace metal composition of marine phytoplankton. *Ann. Rev. Mar. Sci.* **5**: 191–215. doi:[10.1146/annurev-marine-121211-172322](https://doi.org/10.1146/annurev-marine-121211-172322)
- van den Berg, C. M. G. 1982. Determination of copper complexation with natural organic ligands in seawater by equilibration with MnO₂. Part 2: Experimental procedures and application to surface seawater. *Mar. Chem.* **11**: 323–342. doi:[10.1016/0304-4203\(82\)90029-9](https://doi.org/10.1016/0304-4203(82)90029-9)
- van den Berg, C. M. G. 1995. Evidence for organic complexation of iron in seawater. *Mar. Chem.* **50**: 139–157. doi:[10.1016/0304-4203\(95\)00032-M](https://doi.org/10.1016/0304-4203(95)00032-M)
- van Leeuwe, M. A., and J. Stefels. 1998. Effects of iron and light stress on the biochemical composition of Antarctic *Phaeocystis* sp. (Prymnesiophyceae). II. Pigment composition. *J. Phycol.* **34**: 496–503. doi:[10.1046/j.1529-8817.1998.340496.x](https://doi.org/10.1046/j.1529-8817.1998.340496.x)
- van Leeuwe, M. A., and J. Stefels. 2007. Photosynthetic responses in *Phaeocystis Antarctica* towards varying light and iron conditions. *Biogeochemistry* **83**: 61–70. doi:[10.1007/s10533-007-9083-5](https://doi.org/10.1007/s10533-007-9083-5)
- Wolf-Gladrow, D. A., U. Riebesell, S. Burkhardt, and J. Bijma. 1999. Direct effects of CO₂ concentration on growth and isotopic composition of marine plankton. *Tellus Ser. B-Chem. Phys. Meteorol.* **51**: 461–476. doi:[10.1034/j.1600-0889.1999.00023.x](https://doi.org/10.1034/j.1600-0889.1999.00023.x)
- Wright, S. W. and others 1991. Improved HPLC method for the analysis of chlorophylls and carotenoids from marine-phytoplankton. *Mar. Ecol. Prog. Ser.* **77**: 183–196. doi:[10.3354/meps077183](https://doi.org/10.3354/meps077183)
- Xu, K., F. X. Fu, and D. A. Hutchins. 2014. Comparative responses of two dominant Antarctic phytoplankton taxa to interactions between ocean acidification, warming, irradiance, and iron availability. *Limnol. Oceanogr.* **59**: 1919–1931. doi:[10.4319/lo.2014.59.6.1919](https://doi.org/10.4319/lo.2014.59.6.1919)
- Yang, G. Y., and K. S. Gao. 2012. Physiological responses of the marine diatom *Thalassiosira pseudonana* to increased pCO₂ and seawater acidity. *Mar. Environ. Res.* **79**: 142–151. doi:[10.1016/j.marenvres.2012.06.002](https://doi.org/10.1016/j.marenvres.2012.06.002)

Acknowledgments

The authors thank T. Brenneis for laboratory assistance, C. Völkner for voltammetric measurement, and D. Wilhelms-Dick for ICP-MS measurement. Thanks also to K. Bischof and B. Meier-Schlosser for the pigment analysis. F.K. and S.T. were funded by the Helmholtz Association (HGF Young Investigators Group EcoTrace, VH-NG-901) and SB was funded by the Deutsche Forschungsgesellschaft (SPP1158, BE5105/1-1). Finally, the authors thank the members of the Marine Biogeosciences section at the Alfred Wegener Institute for diverse logistical support.

Conflict of Interest

None declared.

Submitted 19 December 2017

Revised 18 June 2018

Accepted 20 August 2018

Associate editor: Heidi Sosik